



1 A searchable database and mass spectral comparison tool for aerosol 2 mass spectrometry (AMS) and aerosol chemical speciation monitor 3 (ACSM)

4 Sohyeon Jeon¹, Michael J. Walker¹, Donna T. Sueper^{2,3}, Douglas A. Day², Anne V. Handschy², Jose L.
5 Jimenez², Brent J. Williams¹

6

7 ¹Department of Energy, Environmental and Chemical Engineering, Washington University in St. Louis, St. Louis, MO, USA

8 ²Department of Chemistry, and Cooperative Institute for Research in Environmental Sciences (CIRES), University of
9 Colorado, Boulder, CO, USA

10 ³Aerodyne Research Inc, Billerica, MA

11

12 *Correspondence to:* Brent J. Williams (brentw@wustl.edu)

13 **Abstract.** The Aerodyne Aerosol Mass Spectrometer (AMS) and Aerosol Chemical Speciation Monitor (ACSM) are the most
14 widely applied tools for in-situ chemical analysis of the non-refractory bulk composition of fine atmospheric particles. The
15 mass spectra (MS) of many AMS and ACSM observations from field and laboratory studies have been reported in peer-
16 reviewed literature and many of these MS have been submitted to an open-access website. With the increased reporting of such
17 data sets, the database interface requires revisions to meet new demands and applications. One major limitation of the web-
18 based database is the inability to automatically search the database and compare previous MS with the researcher's own data.
19 In this study, a searchable database tool for the AMS and ACSM mass spectral dataset was built to improve the efficiency of
20 data analysis using Igor Pro, consistent with existing AMS and ACSM software. The database tool incorporates the published
21 MS and sample information uploaded on the website. This tool allows the comparison of a target mass spectrum with the
22 reference MS in the database, calculating cosine similarity, and provides a range of MS comparison plots, reweighting, and
23 mass spectrum filtering options. The aim of this work is to help AMS users efficiently analyze their own data for possible
24 source or atmospheric processing features by comparison to previous studies, enhancing information gained from past and
25 current global research on atmospheric aerosol.

26

27 1. Introduction

28 Atmospheric aerosol particles have adverse effects on human health and impact visibility, the hydrological cycle, and
29 climate changes through direct and indirect radiative properties (Ramanathan et al., 2001; Bäumer et al., 2008; Kampa and
30 Castanas, 2008; IPCC, 2021). Globally, the dominant constituent of dry fine-mode respirable aerosol particles is organic matter
31 (OM), commonly referred to as organic aerosol (OA). Understanding the characteristics, sources, and processes of OA is key
32 in developing aerosol-related control policies and air quality and climate models. However, OA is chemically complex, with
33 thousands of different compounds detected in single samples (Goldstein and Galbally, 2007). The compositional complexity
34 of OA arises from diverse primary sources and reactions of organic species in the atmosphere that produce secondary OA
35 (SOA) material from gas-to-particle conversion or chemically aged OA (De Gouw and Jimenez, 2009).

36 Aerosol Mass Spectrometry (AMS) has widely been applied to atmospheric science research for analysis of the bulk
37 chemical composition of fine particles. It allows one to measure the non-refractory components of the particles with high time
38 resolution, most typically reporting mass concentrations of total fine OA, sulfate, nitrate, ammonium, and chloride (e.g. Jayne
39 et al., 2000; Jimenez et al., 2003; Allan et al., 2004; DeCarlo et al., 2006; Canagaratna et al., 2007; Baltensperger et al., 2010).
40 The AMS has frequently been used in both field and laboratory studies. In field studies, the AMS has characterized atmospheric
41 particles in environments such as urban, rural, remote, forested, ocean, and agricultural regions (e.g. Allan et al., 2004, 2006;
42 Phinney et al., 2006; Aiken et al., 2009; He et al., 2011; Bates et al., 2012; Cleveland et al., 2012; Dall'Osto et al., 2013; Hao
43 et al., 2014; Xu et al., 2014; Lee et al., 2015; Modini et al., 2015; Xu et al., 2015; Young et al., 2016; Kim et al., 2017). In
44 addition, AMS has been used on many platforms such as mobile labs, aircraft, and ships as well as stationary sites (e.g. Bahreini

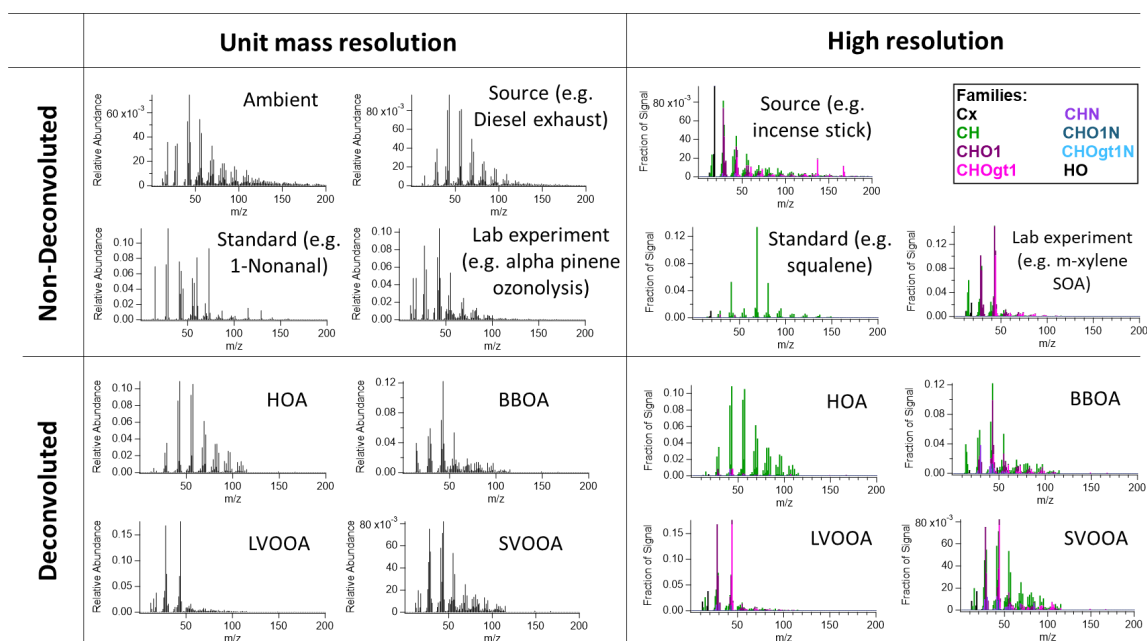


45 et al., 2003; Zorn et al., 2008; Mohr et al., 2011; Coggon et al., 2012; Drewnick et al., 2012; Claeys et al., 2017; Pirjola et al.,
46 2017; Robinson et al., 2018; Shilling et al., 2018). For laboratory studies, particles generated from a variety of sources,
47 including wood burning, cooking, trash burning, coal and fuel combustion, etc., have been characterized using AMS (e.g.
48 Canagaratna et al., 2004; Schneider et al., 2006; Aiken et al., 2008; Weimer et al., 2008; Mohr et al., 2009; Chirico et al., 2010;
49 He et al., 2010; Adam et al., 2011; Heringa et al., 2011; Wang et al., 2013; Collier et al., 2015; Fortenberry et al., 2018).
50 Furthermore, AMS has been employed to analyze SOA formed from different oxidation experiments using environmental
51 chambers or flow tube reactors with varying oxidants, aging processes, concentrations, humidity levels, temperatures,
52 precursors, etc. (e.g. Bahreini et al., 2005; Kroll et al., 2005, 2006; Murphy et al., 2007; Ng et al., 2007, 2008; Chhabra et al.,
53 2010; Lambe et al., 2011, 2012; Loza et al., 2014; Riva et al., 2016; Boyd et al., 2017; Lim et al., 2019).

54 The Aerosol chemical speciation monitor (ACSM) also has been used to analyze the bulk chemical composition of
55 non-refractory components with a very similar sampling and detection technology as the AMS. The key difference is that the
56 ACSM was developed with reduced complexity (e.g. no particle size measurement) and performance (Ng et al., 2011). A major
57 advantage of ACSM over AMS is that it provides a smaller size, lower cost, simpler operation, and less attention from site
58 managers than AMS. In addition, ACSM data are analyzed with the same techniques that are used for the AMS. Therefore, the
59 ACSM has been deployed for long-term monitoring at locations including urban (e.g. Ng et al., 2011; Sun et al., 2011;
60 Budisulistiorini et al., 2013; Carbone et al., 2013; Budisulistiorini et al., 2014; Aurela et al., 2015; Petit et al., 2015;
61 Budisulistiorini et al., 2016; Reyes-Villegas et al., 2016; Rattanavaraha et al., 2017; Sun et al., 2018; Kommula et al., 2021),
62 suburban (Zhang et al., 2018), rural (e.g. Tiitta et al., 2014; Canonaco et al., 2015; Fröhlich et al., 2015a; Parworth et al., 2015;
63 Bressi et al., 2016; Budisulistiorini et al., 2016; Schlag et al., 2016; Zhao et al., 2020), remote (e.g. Budisulistiorini et al., 2015;
64 Fröhlich et al., 2015b; Ripoll et al., 2015; Michoud et al., 2017), and forested areas (e.g. Fröhlich et al., 2013; Minguillón et
65 al., 2015; Heikkinen et al., 2020).

66 According to the broad and diverse application of the AMS and ACSM, data analysis procedures have also been
67 advanced to improve efficiency and accuracy to interpret the data. These advances have made it possible to divide the quantified
68 OA mass concentrations obtained from AMS and ACSM into hydrocarbon-like OA (HOA, a surrogate for primary OA (POA)
69 directly emitted from combustion sources) and oxygenated OA (OOA, a surrogate for SOA generated from a chemical reaction
70 or phase partitioning). Furthermore, OOA can be subdivided into low-volatility OOA (LV-OOA or more-oxidized OOA, MO-
71 OOA) and semi-volatile OOA (SV-OOA or less-oxidized OOA, LO-OOA) when combined with methods such as thermal-
72 denuding inlets and positive matrix factorization (PMF) analysis (Paatero and Tapper, 1994; Zhang et al., 2005; Lanz et al.,
73 2007; Ulbrich et al., 2009; Zhang et al., 2011). In addition, these deconvolved OA have been specifically characterized
74 depending on source types such as biomass burning (BBOA) and cooking (COA), increasing the utility of source apportionment
75 of atmospheric aerosols (Paatero and Tapper, 1994; Ulbrich et al., 2009; Mohr et al., 2009). This improvement in data analysis,
76 in addition to the higher performance and mass spectral resolution of modern time-of-flight (ToF) MS detectors often deployed
77 with the AMS and ACSM, has led to a growing number of reported measurements under various sample configurations and
78 conditions.

79 Mass spectra (MS) from the AMS and ACSM provide powerful information to interpret the OA data. A mass spectrum
80 with specific marker ions, or specific ratios of ions, can often be related to a source or chemical process. Here we broadly
81 classify MS types by mass resolution (unit mass resolution or UMR vs. high mass resolution or HR) and extent of MS separation
82 through data processing (non-deconvoluted/deconvoluted). UMR indicates that the signal at each mass is separated from the
83 next 'integer' m/z . In contrast, HR is able to quantify multiple HR ion fragments at a nominal m/z , which enables more detailed
84 characterization than UMR. DeCarlo et al., (2006) has demonstrated the ability to characterize HR ion fragments below a
85 nominal mass, typically m/z 120. These HR ion fragment signals can be grouped into different ion classes such as C_x , C_xH_y ,
86 $C_xH_yO_z$, etc., which are called 'HR families'. A HR mass spectrum is often plotted in a color-coded stacked bar chart of these
87 HR families. Deconvolution indicates whether or not the MS are generated from an additional analysis step like PMF. If the
88 mass spectrum is obtained from PMF, it is called a 'Deconvoluted' mass spectrum and is identified as HOA, SV-OOA, LV-
89 OOA, etc. If not separated, the mass spectrum is referred to as 'Non-deconvoluted'. A non-deconvoluted MS may be
90 representative of multiple contributing sources or aging processes if an ambient sample or can be a single source or standard
91 observed in a lab study. Figure 1 presents various examples of AMS OA MS classified by resolution and extent of MS
92 processing.



93

94 *Figure 1. Various examples of AMS OA mass spectral data divided by resolution and deconvolution. Each mass spectrum was*
 95 *plotted via the developed AMS MS comparison panel here and original data were from Alfarra et al., (2004); Canagaratna et*
 96 *al., (2004); Katrib et al., (2004); Bahreini et al., (2005); Li et al., (2012); Loza et al., (2012) for non-deconvoluted MS and*
 97 *Mohr et al., (2012) for deconvoluted MS.*

98 With existing datasets growing in complexity and number according to the advancement and accessibility of
 99 technology in the aerosol science field, it is increasingly important to develop customizable databases that store previous
 100 observations and act as a reference for future studies. Previous AMS and ACSM data have often been provided in text and
 101 graphical form, such as peer-reviewed journal publications. However, as the amount of data grows, finding the appropriate data
 102 in a usable format is increasingly challenging. Previous efforts to build a database for AMS and ACSM have been made by
 103 Ulbrich et al., (2009). They collected published AMS and ACSM spectral data and metadata (e.g., instrument operating
 104 conditions, sample, and experiment details), and posted it on an open-access website (<https://cires1.colorado.edu/jimenez-group/AMSsd/>). The digital data was uploaded as an Igor Pro software (Wavemetrics, Portland, OR) text file format, with
 105 an .itx file name extension. This allows users to load or export the data in the Igor Pro software commonly used for AMS and
 106 ACSM data analysis. This is a useful repository to advertise and distribute AMS and ACSM data. However, this repository is
 107 not programmed or formatted to systematically search for appropriate results and compare them with the researcher's own data.
 108 Beyond the need to program a search method, formatting needs to be standardized compared to the current method where each
 109 spectral data is individually uploaded on the webpage with some variability in format (e.g., variable mass-to-charge (m/z)
 110 ranges).
 111

112 In this study, we introduce a searchable database tool for the AMS and ACSM mass spectral dataset. Our aim is to
 113 improve the efficiency and utility of the AMS and ACSM data analysis process, building on the existing database from Ulbrich
 114 et al., (2009). We converted the web-based database to a software-based database format using Igor-pro and developed the Igor
 115 Pro visualization interface. The interface is called 'AMS MS comparison panel' or simply 'panel' in the following sections. To
 116 demonstrate the practical application of this tool, we compared our AMS MS with reference MS in the database. This
 117 comparison demonstrates how our tool can be useful in practical applications. We believe that incorporating this comparison
 118 tool will enhance the ability of AMS and ACSM users to conveniently compare their data with previously reported studies.

119

120 2. Methods

121 The developed database is based on the existing open-access website by Ulbrich et al., (2009), providing published
 122 AMS and ACSM mass spectral datasets. The website mainly consists of 3 separate web pages such as unit mass resolution



123 (UMR, standard vaporizer), high resolution (HR, standard vaporizer), and capture vaporizer (CV, both UMR, and HR). Capture
 124 vaporizer indicates that a more recently developed particle vaporizer was installed, which can lead to different spectra primarily
 125 from increased thermal decomposition (Hu et al., 2018a). For each sample, the website provides metadata in a table format
 126 including spectra identification, sources, research groups, AMS instruments used, electron ionization (EI) energy, and vaporizer
 127 temperature. It also provides citation information and the original figure number in the publication, sometimes with additional
 128 comments. The mass spectrum is uploaded in a digital form for analysis as an .itx file, a plain text file that can be directly
 129 loaded into the data analysis software Igor-pro (Wavemetrics, Portland, OR).

130 Here, to convert this web-based information and individual mass spectrum files to the software-based database in Igor-
 131 Pro, the given information was fetched from HTML using the ‘fetchURL’ function in Igor-Pro to convert the contents of the
 132 HTML to strings. Metadata was extracted from these HTML strings and saved in Igor Pro. Each mass spectrum was
 133 automatically downloaded to the computer first and then saved in the Igor-Pro database. When saving the mass spectrum, it
 134 was aligned and normalized in a uniform format with a consistent m/z range from 1 to 600 and a sum of the spectrum summing
 135 to a value of 1. In the case of high resolution MS, they were converted to a UMR mass spectrum to make the HR mass spectrum
 136 directly comparable to the UMR mass spectrum, and then also saved into the Igor-Pro database. HR ion family data was also
 137 converted to UMR form and saved using the same method. For example, if the HR mass spectrum has three ions as CO_2^+ (m/z
 138 43.9898), $\text{C}_2\text{H}_4\text{O}^+$ (m/z 44.0262), and C_3H_8^+ (m/z 44.0626), all these three ions are considered as m/z 44 on the database panel
 139 in both UMR and HR. However, for HR ion families, these ions are respectively saved to corresponding HR ion families such
 140 as CHOgt1 , CHO1 , and CH (a detailed description of HR families is presented in Table S1). After creating the software-based
 141 database, the visualization interface (i.e., AMS MS comparison panel) was constructed in Igor Pro to analyze the correlation
 142 between MS.

143

144 2.1 Mass spectrum correlation calculation

145 The main goal of this comparison panel is to provide a convenient function to analyze similarities between the mass
 146 spectrum of interest and the reference MS in the database. Cosine similarity is a useful method to estimate mass spectrum
 147 similarity (Stein and Scott, 1994). It has been widely used to analyze the similarity between AMS MS, referring to it as the dot
 148 product with normalized spectra input or uncentered correlation coefficient (e.g. Marcolli et al., 2006; Lambe et al., 2015; Day
 149 et al., 2022). In this comparison tool, cosine similarity (referred to as ‘Cosine score’ on the panel) is used to compare MS. It
 150 measures the cosine of the angle between two vectors and is calculated by using the equation below.

$$151 \quad \text{Cosine score} = \cos(\theta) = \frac{A \cdot B}{\|A\| \|B\|} \quad (\text{Eqn. 1})$$

152 where each vector A and B are corresponding to the mass spectrum of interest and each reference mass spectrum in the database,
 153 respectively. |A| and |B| denote the magnitudes of vectors A and B, and $A \cdot B$ indicates the dot product of A and B. The possible
 154 range of cosine similarity (score) is from 0 to 1, and the higher the score value, the higher the similarity between the MS.

155 In addition, the panel supplies the option to reweight the mass spectrum using Equation 2 below. Regarding the
 156 comparison of MS, instrument operation parameters can cause m/z -dependent differences in the amount or detection of ions,
 157 and preprocessing spectral intensities by reweighting can have a beneficial effect on improving correlations between acquisition
 158 methods (Stein and Scott, 1994). The score can be adjusted by varying their mass weighting and intensity scaling factors.
 159 Increasing the relative significance of the lower-abundance high m/z values can enhance the match-weighting of these more
 160 distinctive ions (i.e., molecular fragments). This is achieved by increasing the mass exponent (mass weighting) or decreasing
 161 the peak intensity exponent (intensity scaling factors) that corresponds to the m and n in Equation 2, respectively.

$$162 \quad \text{Weighted intensity} = [m/z]^m [\text{Peak intensity}]^n \quad (\text{Eqn. 2})$$

163 The weighted exponents default to $m=0$ and $n=1$ on the panel. After reweighting, the mass spectrum is normalized by dividing
 164 each value by the sum of the reweighted mass spectrum (thus summing to unity again). Finally, the panel calculates the score
 165 using the scaled mass spectrum.

166 For HR mass spectral data, the score can be calculated with only the selected HR families on the panel. For example,
 167 if one selects three HR families out of 17, then it combines these three HR family MS of interest into one mass spectrum and
 168 sums to unity for normalization. It then calculates the score with a normalized mass spectrum utilizing the same method
 169 described above. Detailed HR family information will be described in the next section. This score is referred to as ‘Score with
 170 HR family’ on the HR data comparison tab of the panel.

171

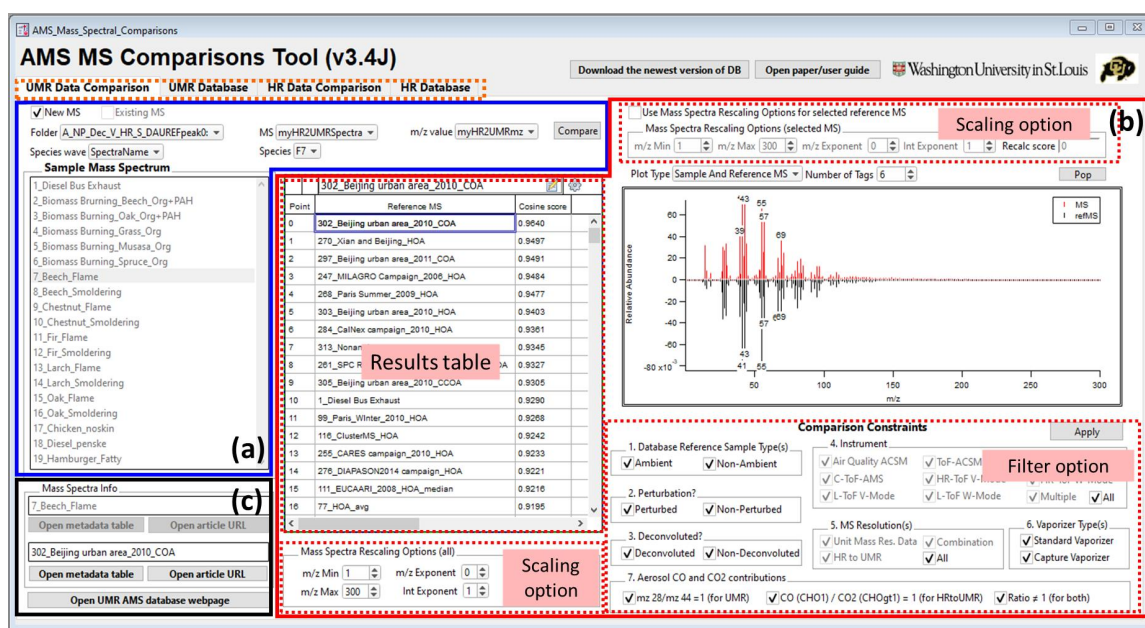


172 2.2 Igor AMS mass spectral comparison panel

173 2.2.1 Data Comparison tab

174 Figure 2 shows a screenshot of the AMS MS comparison panel. The panel is divided into four tabs (dashed line in
 175 orange of Figure 2): i) UMR Data comparison, ii) UMR Database, iii) HR Data comparison, and iv) HR Database. Both data
 176 comparison tabs for UMR and HR data consist of three regions. Figure panel section 2a (highlighted in blue) is where a new
 177 or existing mass spectrum is selected for comparison against database MS. Section 2b (highlighted in red) is where the user
 178 will set search parameters and view results, and section 2c (highlighted in black) is where metadata of selected database
 179 components can be viewed. Screenshots of other tabs are shown in the supplementary material (Figs. S1-3).

180



181

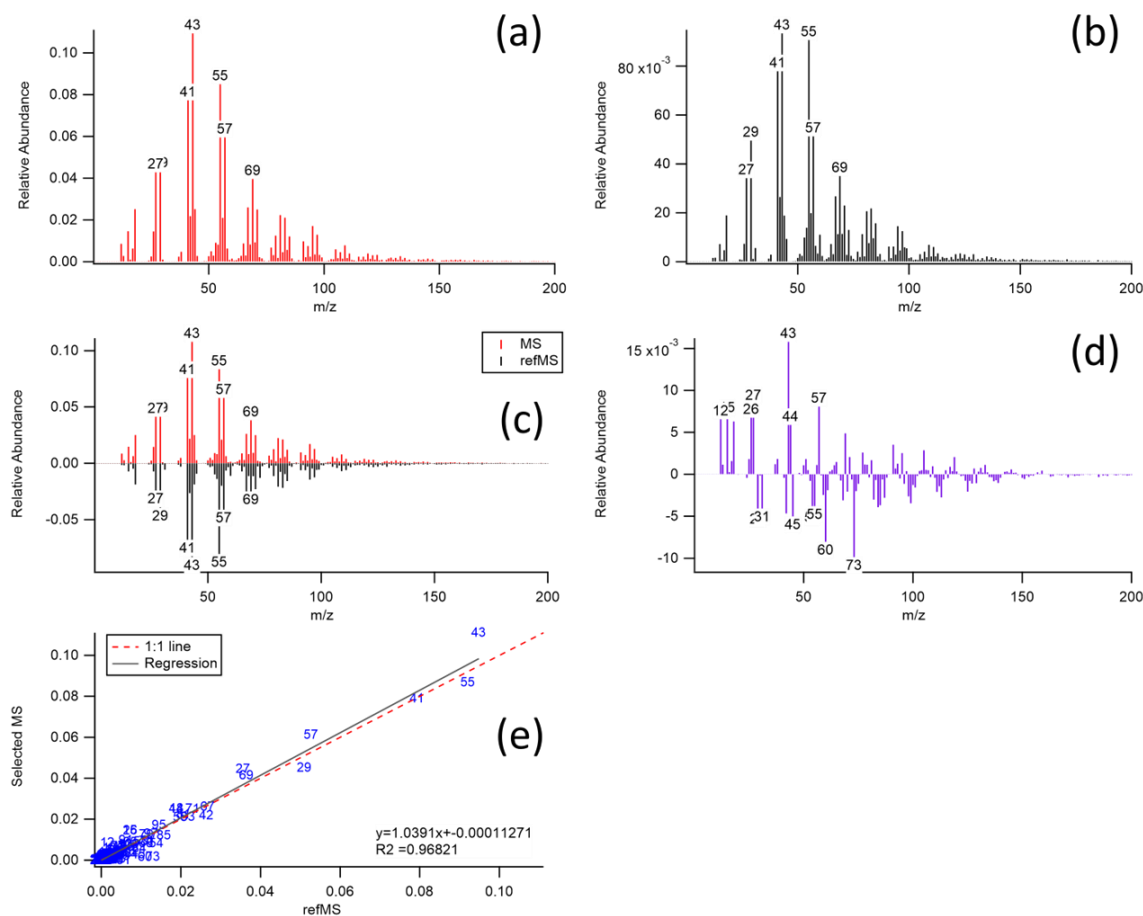
182 Figure 2. A screenshot of the UMR Data comparison tab in the ‘AMS MS Comparison Panel’. In box (a), the user selects their
 183 sample mass spectrum of interest, in box (b) the user views a comparison result of the sample with the database reference mass
 184 spectrum and sets the scaling option and filter option, and the box (c) provides the citation information.

185 In panel section 2a, users are able to select MS to be compared. There are two options for users to choose a mass
 186 spectrum of interest. One is to choose their own mass spectrum, and the other is to select an existing mass spectrum in the
 187 database. In the case of selecting their own mass spectrum, the mass spectrum has to be in UMR with a standard m/z range.
 188 The current panel and database use a mass range of m/z 1-600. Detailed information on how to upload the user’s own data to
 189 the database panel is described in the user guide section (Chapter 2 for UMR and Chapter 3 for HR) of the supplementary
 190 information.

191 Panel section 2b contains the results table, mass spectrum plots window, scaling mass spectrum options, and
 192 comparison filter options. The results table shows the list of reference spectra sorted by the calculated score (cosine similarity)
 193 in descending order. Users are able to see the reference spectrum of interest on the mass spectrum plots window by clicking on
 194 the results table. For the UMR data comparison tab, the mass spectrum plot window provides five types of mass spectrum plots
 195 (selectable with the “Plot Type” drop-down above the plot shown in Fig. 2: sample mass spectrum of interest, reference mass
 196 spectrum selected, mirror-image sample and reference MS, subtraction of sample and reference MS, and the scatter plot
 197 between the sample and reference with the markers corresponding to the specific m/z value with regression information (Fig.
 198 3). For the HR data comparison tab, the panel plots a stacked mass spectrum with HR ion families such as Cx, CH, CHO1,
 199 CHOgt1, etc (Fig. S2b). These HR ion families are the same names generated by PIKA v1.23B which is an AMS data analysis
 200 tool for HR (DeCarlo et al., 2006; Sueper, 2021, <https://cires1.colorado.edu/jimenez-group/ToFAMSResources/ToFSoftware/>).
 201 The chemical formula for each HR ion family is described in Table S1. Users can select the HR ion family to be viewed on the
 202 window and can calculate a ‘score with HR family’ with these selected HR families to compare the mass spectrum specifically.



203 These various types of plots will help users visually observe the similarities and differences between the MS. The scaling mass
 204 spectrum option can reset the mass range and reweight the mass spectrum. Users are able to choose whether to apply the scaling
 205 options to all reference MS in the database (below the results table in panel section 2b) or to only one selected reference mass
 206 spectrum on the list (top right of the panel in panel section 2b) in UMR data comparison tab. For HR data, it only provides the
 207 scaling option for all reference MS. Furthermore, the panel supplies comparison constraints to filter the reference MS in the
 208 database depending on the metadata. Comparison constraint categories include sample type, perturbation, deconvolution,
 209 instrument, MS resolution, and CO and CO₂ contribution sections. Detailed descriptions of these constraints are provided in
 210 the supplementary material (Section S1).



211

212 *Figure 3. Five types of plots provided by the panel to inform mass spectral comparisons: (a) sample mass spectrum of interest,*
 213 *(b) reference mass spectrum selected, (c) mirrored-image sample and reference MS, (d) subtraction (difference) of sample and*
 214 *reference MS, and (e) scatter plot between the sample and reference mass spectrum with the markers corresponding to the*
 215 *specific m/z values with regression information. Original data were from Ulbrich et al., (2009) and Mohr et al., (2009). In this*
 216 *example (as observed in panel d) the sample MS (HOA) contains additional m/z 43 and 57 (both of which have primary or*
 217 *secondary contributions and would need to further explore the HR results to distinguish), and the reference MS (laboratory,*
 218 *chicken cooking without skin) contains additional m/z 60 and 73 (common biomass markers or carboxylic acids).*

219

220 Finally, in panel section 2c, users can find detailed information on the sample mass spectrum of interest and selected
 221 reference MS in the results table. The “Open metadata table” button in panel section 2c enables a new window to pop up for
 222 users to obtain information. The new window shows sample type, perturbed type, analysis, instrument type, resolution,
 223 vaporizer type, EI energy value, vaporizer temperature, experimenter’s name, group, citations, citation URLs, figure numbers



224 in the citation, and related comments (Fig. S4). In addition, users can directly open the relevant published paper in a web
 225 browser via the panel (“Open article URL” button in panel section 2c) if the URL address of the paper is saved in the database.

226

227 2.2.2 Database tab

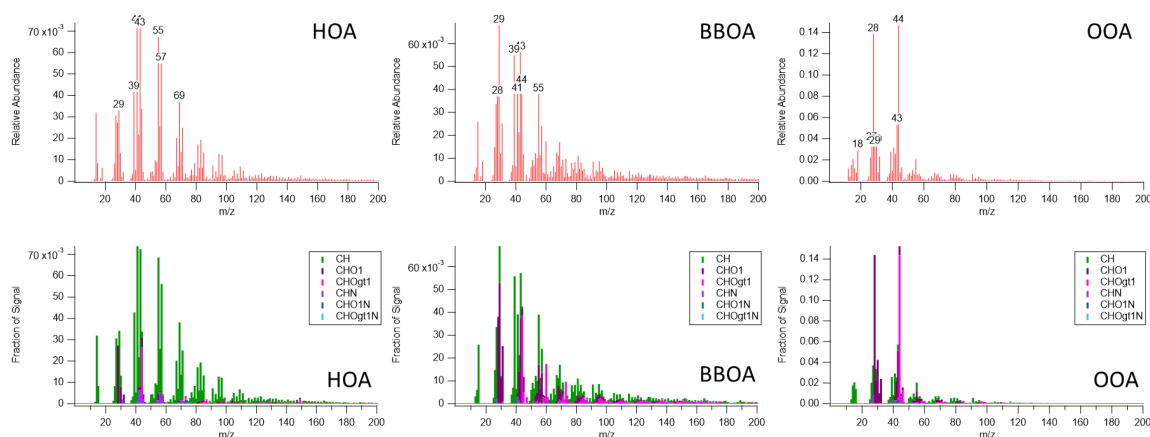
228 Both database tabs of UMR and HR (Figs. S1, S3) display reference MS in the database. Users can simply observe
 229 the reference mass spectrum in the database with metadata without correlation calculation. Users can scan the MS stored in the
 230 database through this tab and easily obtain the corresponding reference metadata.

231

232 **3. Application of the AMS MS database and comparison panel**

233 Here, we used PMF factor mass spectral data from the DAURE campaign (Determination of the sources of
 234 atmospheric Aerosols in Urban and Rural Environments) to display the utility of the developed database and comparison panel.
 235 Data for this study were acquired in high resolution during the intensive DAURE field campaign in Montseny, Spain, during
 236 February-March 2009. An 8-factor solution (FPEAK=0) was chosen since this was the lowest number of factors at which the
 237 HOA and BBOA factors showed a clear separation from each other and OOA. Six factors were recombined to make up the
 238 OOA factor. The BBOA and HOA factors used here are those from the 8-factor solution. More details about an overview of
 239 the DAURE campaign and a summary of the results can be found in Minguillón et al., (2011), Pandolfi et al., (2014), and
 240 Zhang et al., (2022). For comparison, the acquired PMF factor mass spectral data in HR was converted to a UMR mass
 241 spectrum. Figure 4 shows the converted PMF factor MS of HOA, BBOA, and combined OOA in UMR and stacked HR ion
 242 families, respectively. In this section, we will introduce examples of ways to utilize the new comparison panel by applying
 243 functions via the UMR data comparison tab and present a potential for the HR data comparison tab based on HR families and
 244 ‘score with HR family’ to obtain more information to interpret the data depending on our factor MS.

245



246

247 *Figure 4. PMF factor MS from Montseny, Spain during the DAURE campaign (Minguillón et al., 2011) in UMR and stacked*
 248 *HR ion families. The acquired PMF factor MS in high resolution were converted to a UMR mass spectrum and plotted by the*
 249 *AMS MS comparison panel here.*

250

251 As introduced above, the developed database panel provides different ways to compare the MS with filtering or scaling
 252 options. Among these options, the ‘sample type’ category in the filtering option (Fig. 2. section b) enables researchers to select
 253 ‘ambient’ or ‘non-ambient’ samples in the database. The ‘Ambient’ option indicates direct measurement of ambient air and the
 254 ‘non-ambient’ option includes analysis of chamber studies, source emission studies, standards, etc. The scaling option is used
 255 to scale the mass spectrum using the mass range, mass exponent, and intensity exponent based on Eqn. 2. The default setting
 256 of the scaling option on the panel is $m=0$ and $n=1$ on Eqn. 2. The comparison process and results for each method will be
 257 described in this section with the DAURE campaign PMF factor MS as an example.



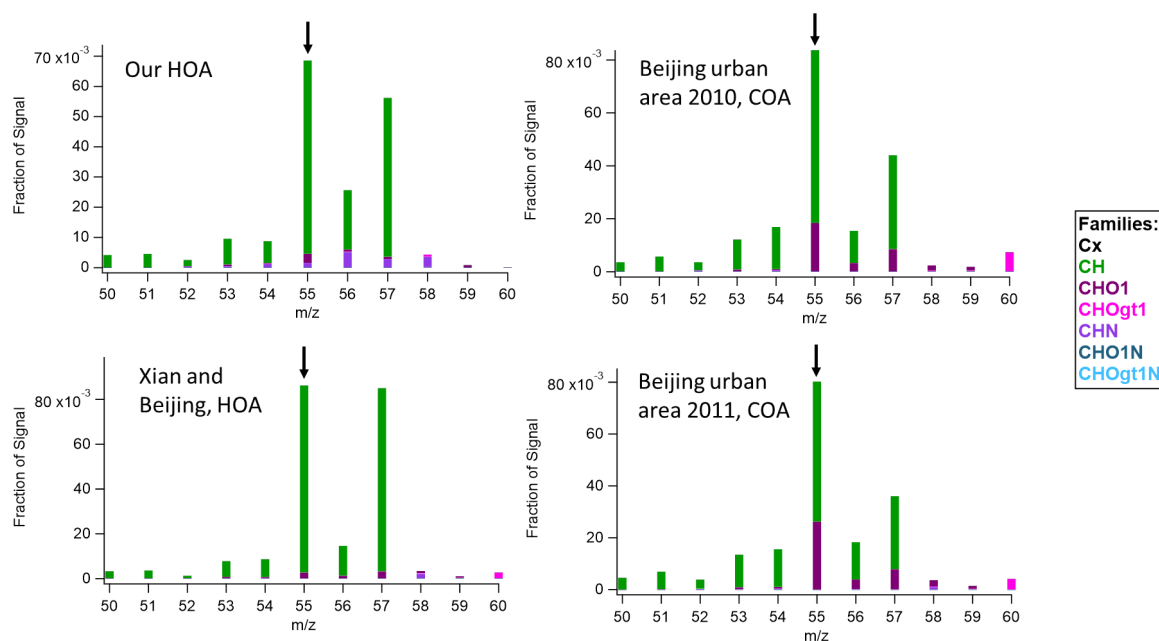
258 Selecting the ‘ambient’ option is useful when the user wants to compare their mass spectrum only with previous
 259 ambient measurements. For example, after the final PMF factors are identified, we may want to confirm if the identified PMF
 260 factors have a similar MS compared with previous studies. In this case, users can apply the ‘ambient’ sample filter to compare.
 261 Table 1 shows the comparison results with the cosine similarity when we executed a UMR comparison of the HOA factor
 262 identified from the DAURE campaign (Montseny, Spain) with the database as an example. In the results table, most of the
 263 samples in the database with a score greater than 0.9 were shown as ‘HOA’. An interesting observation that appears is that
 264 some cooking organic aerosol (COA) factors also showed a high correlation with our HOA factor. The COA factor is often
 265 identified by its characteristic mass fragment of m/z 55, and it also has the same hydrocarbon ion series (m/z 29, 43, 57, 71, for
 266 $C_nH_{2n+1}^+$ and m/z 41, 55, 69, for $C_nH_{2n-1}^+$) as the HOA (Mohr et al., 2009). The HOA factor we compared has a large m/z 55
 267 in the spectrum and that may be the main cause for some COA factors to score a high match. Therefore, we would conclude
 268 that our HOA factor might be mixed with cooking sources. However, in this case, if the user has HR family information of the
 269 mass spectrum, as we do here, one could have more information to interpret the result.

270 COA factor MS usually have a relatively high portion of CHO1 family in m/z 55 compared to HOA, which would be
 271 from the $C_3H_3O^+$ ion (Mohr et al., 2009, 2012). Figure 5 shows the comparisons of m/z 55 in stacked HR families with the top
 272 3 reference samples in Table 1. The m/z 55 in our HOA and Xian and Beijing HOA factor MS mainly consists of CH family,
 273 specifically $C_4H_7^+$, and this contribution is clearly distinguished from the COA reference MS such as Beijing urban area 2010
 274 and 2011 having larger m/z 55 contributions from CHO1 family, specifically $C_3H_3O^+$. These trends are also shown in Mohr et
 275 al., (2012) where AMS data acquired during the field campaign DAURE in Barcelona, Spain were analyzed and HOA and
 276 COA were both separated as a result. The HOA factor mass spectrum in Mohr et al., (2012) also had the m/z 55 only slightly
 277 smaller than m/z 57. However, the m/z 55 in their HOA factor mass spectrum is also predominantly contributed from the CH
 278 family as we observed here. Likewise, in their COA factor mass spectrum, m/z 55 is much larger than m/z 57 and nearly half
 279 of m/z 55 was from the CHO1 family. Therefore, we may conclude that our HOA factor is most similar to previous ‘HOA’ MS
 280 even if it has a high abundance of m/z 55. However, it also suggested that additional PMF analysis with more factors could find
 281 some contribution of COA mixed in our HOA that could perhaps be separated. This comparison shows the strength of
 282 incorporating the HR families available from HR-AMS datasets as well as simple UMR ambient comparison via the panel.

283 *Table 1. Top matches from “Ambient” sample UMR comparison results with HOA factor from the DAURE campaign (m/z 1-*
 284 *200)*

# in DB	Sample	Score	Reference
311	Beijing urban area_2010_COA	0.9640	(Hu et al., 2016)
279	Xian and Beijing_HOA	0.9497	(Elser et al., 2016)
306	Beijing urban area_2011_COA	0.9492	(Hu et al., 2016)
253	MILAGRO Campaign_2006_HOA	0.9483	(Alfarra et al., 2004)
277	Paris Summer_2009_HOA	0.9477	(Crippa et al., 2013)
312	Beijing urban area_2010_HOA	0.9403	(Hu et al., 2016)
293	CalNex campaign_2010_HOA	0.9361	(Hayes et al., 2013)
270	SPC Research Station Po Valley_2008_HOA	0.9327	(Saarikoski et al., 2012)
314	Beijing urban area_2010_CCOA	0.9305	(Hu et al., 2016)
101	Paris_Winter_2010_HOA	0.9269	(Crippa et al., 2013)

285



286

287 *Figure 5. Segments of the MS (m/z 50-60) for our HOA and top 3 reference samples that correlated highly with our HOA in*
 288 *the “Ambient” comparison for m/z 55 HR ion families*

289

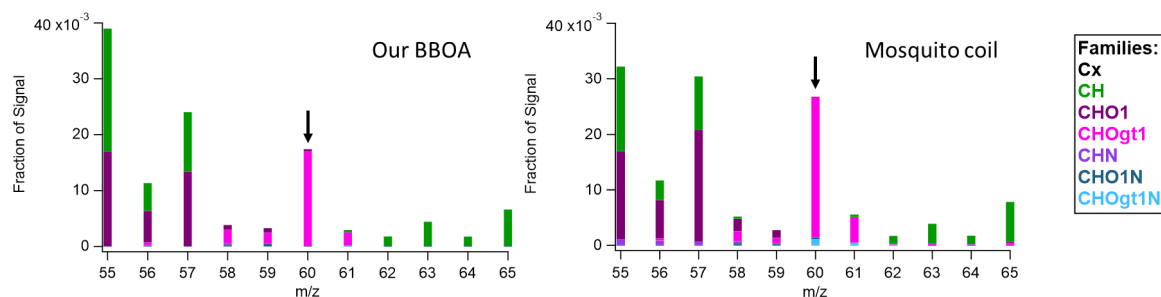
290 ‘Non-ambient’ option is convenient to compare the mass spectrum of interest with laboratory samples in the database.
 291 For example, this option is helpful when comparing a mass spectrum derived from a specific source such as BBOA. When
 292 applying the non-ambient filtering option, several non-ambient reference MS were highly correlated with our BBOA MS (Table
 293 2). The characteristic mass fragment of BBOA is m/z 60 attributed to $C_2H_4O_2^+$ (from anhydrous sugars such as levoglucosan)
 294 and this specific ion was observed in most of the MS in the list of high score matches. On the HR data comparison tab, we are
 295 able to confirm if the m/z 60 is from the oxygenated HR family (CHOgt1). In Table 2, only the mosquito coil sample included
 296 HR ion family data and we confirmed the m/z 60 was mostly from CHOgt1 ion family which is pink (Fig. 6). Since the main
 297 component of mosquito coil is biomass such as sawdust, coconut shell flour, pyrethrum, potato starch, etc, it seems to show a
 298 high correlation with our BBOA and similar HR ion family contribution in m/z 60.

299

300 *Table 2. Top matches from “Non-ambient” sample UMR comparison results with the BBOA factor from the DAURE*
 301 *campaign (m/z 1-200)*

# in DB	Sample	Score	Reference
30	Ponderosa Pine Duff	0.9404	
41	Puerto Rican Mixed Wood	0.9337	(FLAME)
40	Southern Pine Needles	0.9335	
325	Mosquito Coil	0.9303	(Li et al., 2012)
38	Puerto Rican Fern	0.9296	
31	Alaska Core Tundra Duff	0.9275	
36	Ceanothus Leaves and Berries	0.9193	
27	Ponderosa Pine Needles and Sticks	0.9184	(FLAME)
39	Wax Myrtle	0.9038	
35	Lignin Powder	0.8951	

302



303
304

Figure 6. Enlarged MS of our BBOA and mosquito coil sample for m/z 60 HR ion family

305

306

An interesting observation from BBOA example is that when carrying out the ambient sample comparison with the BBOA factor, other identifications such as HOA, SVOOA, LOOOA, COA, etc were observed as well as BBOA (Table 3) even though our BBOA mass spectrum was highly correlated with biomass burning laboratory references. Since ion separation of AMS mass spectrum via PMF is largely impacted by the mix of sources present at a given time, users don't always obtain a 'perfectly separated' mass spectrum identifying the mass spectrum as HOA, BBOA, COA, etc, but a possibly mixed mass spectrum. It indicates that even if the UMR score on the panel is lower, it could be possible that there is a good match with a single HR family or some families, and vice versa. For this case, 'Score with HR family' can be a useful function to gain more information on similarities. When users select the HR families of interest next to the HR plot window and click the calculate button below HR family selection, it combines only the selected HR families into one MS, calculates a cosine similarity in the same way, and displays the results named 'score with HR family' on the results table. Table 3 shows top 10 matches from ambient sample comparison results sorted by the UMR score and top 10 matches from 'score with HR family'. For BBOA, the separation of the oxygenated ions provides a lot of information and is a key signature of BBOA spectra. On Table 3, we were able to observe more BBOA factor mass spectrum on the list when sorting the results by the score with CHOg1 family including m/z 60. Most of the new matches showed BBOA, CCOA (coal combustion OA), HOA, and COA, not OOA like when sorting the list by UMR score. UMR match scores for these reference MS are included alongside the HR Family match score for comparison. We also carried out a score comparison utilizing additional HR families and family combinations (CH, CHO1, and combined), but it did not provide additional insight beyond what was observed with CHOg1 alone (Table S2).

323

324
325

Table 3. Top matches from HR "Ambient" sample comparison results with the BBOA factor from the DAURE campaign (m/z 1-200) depending on UMR score and score with HR family (CHOg1)

Top 10 matches sorted by UMR score				
# in DB	Sample	UMR score	Reference	
293	Changdao island_2011_biomass burning	0.9632	(Hu et al., 2013)	
310	SOAS campaign_2013_SOA	0.9445	(Hu et al., 2015)	
300	Beijing urban area_2011_HOA	0.9367	(Hu et al., 2016)	
245	SOAR-1_Campaign_2005_SVOOA	0.9346	(Docherty et al., 2011)	
313	SOAS campaign_2013_LOOOA_II	0.9287	(Hu et al., 2015)	
296	Changdao island_2011_CCOA	0.9239	(Hu et al., 2013)	
315	KORUS-AQ study_2016_LOOOA	0.9164	(Hu et al., 2018b)	
269	Paris Summer_2009_SVOOA	0.9149	(Crippa et al., 2013)	
301	Beijing urban area_2011_COA	0.9097	(Hu et al., 2016)	
265	SPC Research Station Po Valley_2008_HOA	0.9050	(Saarikoski et al., 2012)	
Top 10 matches sorted by the score with HR family (CHOg1)				
# in DB	Sample	UMR score	Score with CHOg1	Reference
254	DAURE campaign_2009_BBOA	0.8348	0.9527	(Mohr et al., 2012)



296	Changdao island_2011_CCOA	0.9239	0.9265	(Hu et al., 2013)
259	CARES campaign_2010_HOA	0.8384	0.9216	(Setyan et al., 2012)
268	Paris Summer_2009_COA	0.8231	0.9208	(Crippa et al., 2013)
275	Xian and Beijing_COA	0.8311	0.9195	(Elser et al., 2016)
283	POPE2014 campaign_COA	0.7947	0.9079	(Struckmeier et al., 2016)
266	SPC Research Station Po Valley_2008_BBOA	0.8913	0.9061	(Saarikoski et al., 2012)
304	Beijing urban area_2010_LVOOA	0.8474	0.9052	(Hu et al., 2016)
293	Changdao island_2011_biomass burning	0.9632	0.9045	(Hu et al., 2013)
307	Beijing urban area_2010_HOA	0.8496	0.8995	(Hu et al., 2016)

326

327 Lastly, users can use the “scaling mass spectrum” feature, which is especially helpful for up-weighting signal intensity
 328 of larger and more unique ions by increasing the mass exponent value or decreasing the intensity exponent value. When we
 329 compared the OOA factor MS with ambient samples, we observed that our OOA factor MS was highly correlated with LVOOA
 330 (or MOOOA) MS from previous studies (Table S3) showing a score of more than 0.97. We also explored cosine scores of the
 331 OOA factor with non-ambient spectra within the database. However, when we compared the OOA factor MS with non-ambient
 332 samples, top scores in the list were shown as less than 0.9 (Table 4). For OOA, the abundances of fragment ions m/z 28 (CO^+)
 333 and 44 (CO_2^+) are extremely dominant compared to other ions in the mass spectrum (typically, the m/z 28 signal is constrained
 334 to be equal to the m/z 44 signal). These prominent abundances of a few spectral peaks may affect score calculation. In the case
 335 of ‘ambient’ comparison with deconvoluted MS dominated by m/z 28 and 44, signals from other ions may not highly influence
 336 the results as shown in Table S3. On the other hand, in the case of ‘non-ambient’ comparison with non-deconvoluted MS
 337 dominated by m/z 28 and m/z 44 signals of laboratory samples, signals from other ions are more unique to the specific laboratory
 338 conditions and may reflect the lower scores as shown in Table 4. In this case, we have two options to reduce these impacts on
 339 score results: i) increase the m/z exponent value, ii) decrease the intensity exponent value, or iii) both i and ii in Eqn 2.

340

341 *Table 4. Top matches from UMR “Non-ambient” sample comparison results with the OOA factor from the DAURE*
 342 *campaign (default setting, m/z 1-200)*

# in DB	Sample	Score	Reference
141	Oxalic acid	0.8493	(Takegawa et al., 2007)
334	Chamber m-Xylene aged SOA	0.8458	(Loza et al., 2012)
321	Incense Coil	0.8385	(Li et al., 2012)
145	Adipic acid	0.8196	(Takegawa et al., 2007)
149	Glyoxylic acid	0.8132	(Takegawa et al., 2007)
331	Citric Acid (C6H8O7)	0.7661	(Hu et al., 2018b)
143	Succinic acid	0.7649	(Takegawa et al., 2007)
234	Diesel_Exhaust_2	0.7629	(Sage et al., 2008)
322	Mosquito Coil	0.7580	(Li et al., 2012)
333	Chamber m-Xylene peak growth SOA	0.7529	(Loza et al., 2012)

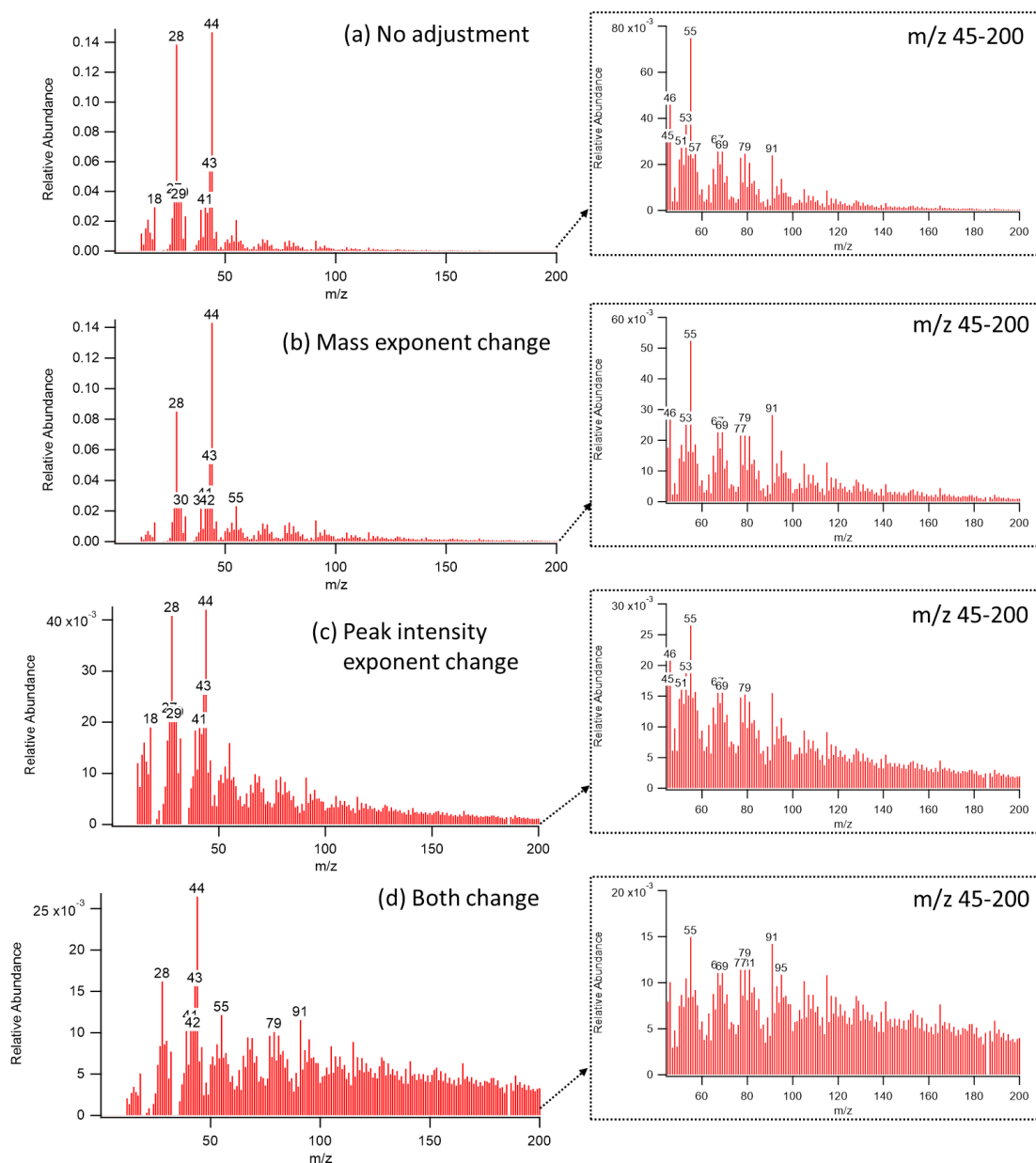
343

344

345 Figure 7 shows the reweighted OOA mass spectrum generated by two exponent options. When we increased the m/z
 346 exponent from 0 to 1 (Figure 7b), we observed that the relative abundance of lower mass fragments decreased and that of larger
 347 mass fragments increased in a similar scale of relative abundance as the original MS (Figure 7a). When we decreased the peak
 348 intensity exponent from 1 to 0.5 (Figure 7c), the maximum value of relative abundance was decreased. Signal intensities other
 349 than the dominant fragments (m/z 28 and 44) were more balanced than in Figure 7a. Figure 7d is the case where we applied
 350 both mass and peak intensity exponent options. It shows the reweighted spectra with relatively smaller contributions from lower
 351 masses and higher contributions from larger masses. Table 5 shows the list of reference MS with a high correlation with our
 352 reweighted OOA factor MS with various pairs of m/z and peak intensity exponent. The scores less than 0.9 were not shown in
 353 the table and the reference samples were sorted by the maximum score among the values from each scenario. It shows that for
 354 our OOA factor MS, decreasing the intensity exponent option resulted in more scores greater than 0.9 compared to increasing
 355 the m/z exponent. Also, we observed that the reweighted OOA factor mass spectrum is mostly correlated with coils, terpene



356 ozonolysis, aged SOA, etc. Correlations to the coils may be because both incense coil and mosquito coil have fragrances that
 357 contain aromatic compounds that can produce oxygenated aromatics during combustion.



358 *Figure 7. The reweighted mass spectrum of DAURE OOA factor ((a): No adjustment, (b): increase m/z exponent from 0 to 1,*
 359 *(c): decrease intensity exponent from 1 to 0.5, and (d): apply (b) and (c) simultaneously). Enlarged mass spectrum with a*
 360 *restricted mass range (m/z 45-200) shown in the dashed line box.*

361

362



363 *Table 5. Top matches from “Non-ambient” UMR sample comparison results with the OOA factor from the DAURE campaign*
 364 *depending on decreasing peak intensity exponent and increasing mass exponent. The maximum score is shown in bold.*

		<i>m/z</i> exponent	0	1	1	
		Peak intensity exponent	0.5	1	0.5	
# in DB	Sample		Score		Reference	
321	Incense Coil		0.9413	-	0.9316	(Li et al., 2012)
334	Chamber m-Xylene aged SOA		0.9306	-		(Loza et al., 2012)
212	Myrcene_O3		-	-	0.9252	(Bahreini et al., 2005)
322	Mosquito Coil		0.9149	-	0.9199	(Li et al., 2012)
222	Myrcene_O3		-	-	0.9176	(Bahreini et al., 2005)
32	Utah Sage, Rabbitbrush		-	-	0.9174	(FLAME, 2007)
213	Terpinolene_O3		-	-	0.9157	(Bahreini et al., 2005)
31	Utah Juniper Foliage and Sticks		-	-	0.9151	(FLAME, 2007)
205	beta-caryophyllene_O3		-	-	0.9151	(Bahreini et al., 2005)
130	Fulvic Acid		-	-	0.9142	(Alfarra, 2004)

365

366 Setting a restricted mass range is another way to modify the score. Table 6 shows the scores of our reweighted OOA
 367 MS when setting a new mass range from *m/z* 45 to 200 and changing the mass and the peak intensity exponent, respectively.
 368 Increasing the mass range parameter was generally helpful to explore comparisons beyond the dominant *m/z* 28 and *m/z* 44
 369 signals. Decreasing the peak intensity exponent showed higher scores in the list compared to the case of increasing the mass
 370 exponent. However, for our OOA, the mass exponent change was more useful to emphasize specific larger ions such as *m/z*
 371 55, 91, and 115 shown in the enlarged mass spectrum in a dashed box of Figure 7b. We observed that the higher *m/z* range in
 372 the reweighted OOA mass spectrum is highly correlated with terpene ozonolysis and biomass burning (Table 6).

373

374 *Table 6. Top matches from “Non-ambient” sample UMR comparison results with the reweighted OOA factor from the DAURE*
 375 *campaign depending on the pairs of mass and intensity exponent value with restricted mass range (*m/z* 45-200)*

		<i>m/z</i> exponent	0	0	1	1	
		Peak intensity exponent	1	0.5	1	0.5	
# in DB	Sample		Score		Reference		
217	Bcaryophyllene_O3		0.9097	0.9587	0.9292	0.9723	(Bahreini et al., 2005)
32	Utah Sage, Rabbitbrush		0.9052	0.9563	0.9277	0.9696	(FLAME, 2007)
205	beta-caryophyllene_O3			0.9586	0.9264	0.9693	(Bahreini et al., 2005)
212	Myrcene_O3			0.9596	0.9185	0.9693	(Bahreini et al., 2005)
31	Utah Juniper Foliage and Sticks				0.9218	0.9668	(FLAME, 2007)
222	Myrcene_O3			0.9568		0.9667	(Bahreini et al., 2005)
218	a-Humulene_O3		0.9165	0.9578	0.9285	0.9651	(Bahreini et al., 2005)
26	Southern CA Chamise					0.9579	(FLAME, 2007)
203	a-humulene_O3			0.9513	0.9156	0.9538	(Bahreini et al., 2005)
206	beta-pinene_O3		0.9139	0.9538	0.9258		(Bahreini et al., 2005)

376

377 In addition to the comparison of the combined OOA mass spectrum, we used these scaling options to check if each of
 378 the original 6 OOA-related factors had potential characteristics to be identified before they were combined. As a result of the
 379 application of a variety of paired scalings of mass range, mass exponent value, and intensity exponent value, we observed
 380 potential characteristics between factors when using the mass range is *m/z* 45-200 and default exponent value (*m*=0, *n*=1)
 381 (Table S4). In this case, factor 1 and factor 4 were highly correlated with the oxidation of m-xylene (an anthropogenic VOC
 382 common in fossil fuels) and other potential ozonolysis products, and factor 5 and factor 6 were mostly correlated with terpene
 383 ozonolysis. Factor 2 and factor 3 showed relatively lower scores but nitrogen-related MS was shown in the results table in both
 384 factors. These results suggest that we could combine factors 1 and 4, factors 2 and 3, and factors 5 and 6 as potential OOA
 385 subcategories. When we calculated cosine similarities between these pairs of factors, it showed a high correlation with the score
 386 of 0.9576, 0.9469, and 0.9838, respectively, which supports their similarities in composition. Factors 5 and 6, in particular, had
 387 characteristic fragment ion *m/z* 91 which can be indicative of monoterpene oxidation matching the results we obtained.
 388 Therefore, based on a new combination of factors, we may conclude that our OOA may be mainly derived from m-xylene



389 (anthropogenic VOC) oxidation, terpene ozonolysis, and nitrogen-related reactions. For HR data comparison, unfortunately,
390 all non-ambient samples in this match list were originally submitted only in UMR, so HR family comparison was not available
391 in this case. Importantly, future MS submissions from the user community should include HR MS when available.

392

393 **4. Conclusions**

394 The existing AMS and ACSM mass spectral database in web-based form has been converted into a searchable,
395 filterable software library coupled with a comparison panel in Igor Pro, the main analysis program currently used for AMS and
396 ACSM data. The comparison panel provides the functionality to compare the mass spectrum of interest with MS in the database
397 statistically and visually by cosine similarity and several types of mass spectral plots as UMR or stacked HR ion families.
398 Furthermore, the option to exponentially reweight the mass spectrum and filter the samples depending on their measurement
399 information (e.g. lab vs field data) can help users understand and analyze their data relative to a growing list of past
400 observations. We believe this new database can be used to improve the efficiency of data interpretation and provide new insights
401 for AMS and ACSM studies. However, the AMS and ACSM users' network should further populate this digital mass spectral
402 database in order to fully realize the potential strength of such a tool. Users can download the procedure file for this database
403 and search the tool through the GitHub link on the existing AMS database webpage ([https://cires1.colorado.edu/jimenez-](https://cires1.colorado.edu/jimenez-group/AMSsd/)
404 [group/AMSsd/](https://cires1.colorado.edu/jimenez-group/AMSsd/)). Users can also follow the listed procedures for submitting new MS to the database and refer to the user manual
405 (see user guide section in supplementary material) to use this tool. While MS are one of the AMS data to be used for data
406 interpretation, users should continue to consider all supporting chemical and meteorological measurements together with the
407 AMS MS in determining factor identities. Our intention is that this database continues to grow and develop with the various
408 types of AMS systems in operation, and can serve as a valuable tool to help AMS users frame their observations against a
409 wealth of previous observations obtained globally.

410

411 **Code availability**

412 The code of AMS mass spectral database in this study was developed in the Igor Pro environment. The codes are available at
413 https://github.com/ActlabW/AMS_MS_DB.

414

415 **Data availability**

416 AMS mass spectra data used in this study is available at <https://cires1.colorado.edu/jimenez-group/AMSsd/>.

417

418 **Author contribution**

419 SJ developed the software code and prepared the manuscript with constructive feedback from DTS and DAD. MJW
420 conceptualized the project and framed the initial code. DTS and DAD contributed to inspecting the tool and the database. DTS,
421 DAD, AVH, and JLJ supplied AMS mass spectral data of DAURE campaign (Montseny). BJW supervised the project. All
422 authors participated in reviewing and editing the manuscript.

423

424 **Competing interests**

425 The contact author has declared that none of the authors has any competing interests.

426

427 **Acknowledgments**

428 BJW acknowledges NSF CBET (award number 1554061) for supporting this study. DTS, AVH, DAD, JLJ acknowledge
429 support from NASA 80NSSC21K1451 and NSF AGS AGS-2131914 and 2206655.

430



431 **References**

- 432 Adam, T. W., Chirico, R., Clairotte, M., Elsasser, M., Manfredi, U., Martini, G., Sklorz, M., Streibel, T., Heringa, M. F.,
433 DeCarlo, P. F., Baltensperger, U., De Santi, G., Krasenbrink, A., Zimmermann, R., Prevot, A. S. H., and Astorga, C.:
434 Application of Modern Online Instrumentation for Chemical Analysis of Gas and Particulate Phases of Exhaust at the
435 European Commission Heavy-Duty Vehicle Emission Laboratory, *Anal. Chem.*, 83, 67–76,
436 <https://doi.org/10.1021/ac101859u>, 2011.
- 437 Aiken, A. C., DeCarlo, P. F., Kroll, J. H., Worsnop, D. R., Huffman, J. A., Docherty, K. S., Ulbrich, I. M., Mohr, C.,
438 Kimmel, J. R., Sueper, D., Sun, Y., Zhang, Q., Trimborn, A., Northway, M., Ziemann, P. J., Canagaratna, M. R., Onasch, T.
439 B., Alfarra, M. R., Prevot, A. S. H., Dommen, J., Duplissy, J., Metzger, A., Baltensperger, U., and Jimenez, J. L.: O/C and
440 OM/OC Ratios of Primary, Secondary, and Ambient Organic Aerosols with High-Resolution Time-of-Flight Aerosol Mass
441 Spectrometry, *Environ. Sci. Technol.*, 42, 4478–4485, <https://doi.org/10.1021/es703009q>, 2008.
- 442 Aiken, A. C., Salcedo, D., Cubison, M. J., Huffman, J. A., DeCarlo, P. F., Ulbrich, I. M., Docherty, K. S., Sueper, D.,
443 Kimmel, J. R., Worsnop, D. R., Trimborn, A., Northway, M., Stone, E. A., Schauer, J. J., Volkamer, R. M., Fortner, E., de
444 Foy, B., Wang, J., Laskin, A., Shutthanandan, V., Zheng, J., Zhang, R., Gaffney, J., Marley, N. A., Paredes-Miranda, G.,
445 Arnott, W. P., Molina, L. T., Sosa, G., and Jimenez, J. L.: Mexico City aerosol analysis during MILAGRO using high
446 resolution aerosol mass spectrometry at the urban supersite (T0) – Part 1: Fine particle composition and organic source
447 apportionment, *Atmospheric Chemistry and Physics*, 9, 6633–6653, <https://doi.org/10.5194/acp-9-6633-2009>, 2009.
- 448 Alfarra, M. R.: Insights into atmospheric organic aerosols using an aerosol mass spectrometer, PhD Thesis, University of
449 Manchester, 2004.
- 450 Alfarra, M. R., Coe, H., Allan, J. D., Bower, K. N., Boudries, H., Canagaratna, M. R., Jimenez, J. L., Jayne, J. T., Garforth,
451 A. A., Li, S.-M., and Worsnop, D. R.: Characterization of urban and rural organic particulate in the Lower Fraser Valley
452 using two Aerodyne Aerosol Mass Spectrometers, *Atmospheric Environment*, 38, 5745–5758,
453 <https://doi.org/10.1016/j.atmosenv.2004.01.054>, 2004.
- 454 Allan, J. D., Delia, A. E., Coe, H., Bower, K. N., Alfarra, M. R., Jimenez, J. L., Middlebrook, A. M., Drewnick, F., Onasch,
455 T. B., Canagaratna, M. R., Jayne, J. T., and Worsnop, D. R.: A generalised method for the extraction of chemically resolved
456 mass spectra from Aerodyne aerosol mass spectrometer data, *Journal of Aerosol Science*, 35, 909–922,
457 <https://doi.org/10.1016/j.jaerosci.2004.02.007>, 2004.
- 458 Allan, J. D., Alfarra, M. R., Bower, K. N., Coe, H., Jayne, J. T., Worsnop, D. R., Aalto, P. P., Kulmala, M., Hyötyläinen, T.,
459 Cavalli, F., and Laaksonen, A.: Size and composition measurements of background aerosol and new particle growth in a
460 Finnish forest during QUEST 2 using an Aerodyne Aerosol Mass Spectrometer, *Atmospheric Chemistry and Physics*, 6, 315–
461 327, <https://doi.org/10.5194/acp-6-315-2006>, 2006.
- 462 FLAME: <http://chem.atmos.colostate.edu/FLAME/>.
- 463 Aurela, M., Saarikoski, S., Niemi, J. V., Canonaco, F., Prevot, A. S. H., Frey, A., Carbone, S., Kousa, A., and Hillamo, R.:
464 Chemical and Source Characterization of Submicron Particles at Residential and Traffic Sites in the Helsinki Metropolitan
465 Area, Finland, *Aerosol Air Qual. Res.*, 15, 1213–1226, <https://doi.org/10.4209/aaqr.2014.11.0279>, 2015.
- 466 Bahreini, R., Jimenez, J. L., Wang, J., Flagan, R. C., Seinfeld, J. H., Jayne, J. T., and Worsnop, D. R.: Aircraft-based aerosol
467 size and composition measurements during ACE-Asia using an Aerodyne aerosol mass spectrometer, *Journal of Geophysical
468 Research: Atmospheres*, 108, <https://doi.org/10.1029/2002JD003226>, 2003.
- 469 Bahreini, R., Keywood, M. D., Ng, N. L., Varutbangkul, V., Gao, S., Flagan, R. C., Seinfeld, J. H., Worsnop, D. R., and
470 Jimenez, J. L.: Measurements of Secondary Organic Aerosol from Oxidation of Cycloalkenes, Terpenes, and m-Xylene
471 Using an Aerodyne Aerosol Mass Spectrometer, *Environ. Sci. Technol.*, 39, 5674–5688, <https://doi.org/10.1021/es048061a>,
472 2005.
- 473 Baltensperger, U., Chirico, R., DeCarlo, P. F., Dommen, J., Gaeggeler, K., Heringa, M. F., Li, M., Prévôt, A. S. H., Alfarra,
474 M. R., Gross, D. S., and Kalberer, M.: Recent Developments in the Mass Spectrometry of Atmospheric Aerosols, *Eur J Mass
475 Spectrom (Chichester)*, 16, 389–395, <https://doi.org/10.1255/ejms.1084>, 2010.
- 476 Bates, T. S., Quinn, P. K., Frossard, A. A., Russell, L. M., Hakala, J., Petäjä, T., Kulmala, M., Covert, D. S., Cappa, C. D.,
477 Li, S.-M., Hayden, K. L., Nuaaman, I., McLaren, R., Massoli, P., Canagaratna, M. R., Onasch, T. B., Sueper, D., Worsnop,
478 D. R., and Keene, W. C.: Measurements of ocean derived aerosol off the coast of California, *Journal of Geophysical*



- 479 Research: Atmospheres, 117, <https://doi.org/10.1029/2012JD017588>, 2012.
- 480 Bäumler, D., Vogel, B., Versick, S., Rinke, R., Möhler, O., and Schnaiter, M.: Relationship of visibility, aerosol optical
481 thickness and aerosol size distribution in an ageing air mass over South-West Germany, *Atmospheric Environment*, 42, 989–
482 998, <https://doi.org/10.1016/j.atmosenv.2007.10.017>, 2008.
- 483 Boyd, C. M., Nah, T., Xu, L., Berkemeier, T., and Ng, N. L.: Secondary Organic Aerosol (SOA) from Nitrate Radical
484 Oxidation of Monoterpenes: Effects of Temperature, Dilution, and Humidity on Aerosol Formation, Mixing, and
485 Evaporation, *Environ. Sci. Technol.*, 51, 7831–7841, <https://doi.org/10.1021/acs.est.7b01460>, 2017.
- 486 Bressi, M., Cavalli, F., Belis, C. A., Putaud, J.-P., Fröhlich, R., Martins dos Santos, S., Petralia, E., Prévôt, A. S. H., Berico,
487 M., Malaguti, A., and Canonaco, F.: Variations in the chemical composition of the submicron aerosol and in the sources of
488 the organic fraction at a regional background site of the Po Valley (Italy), *Atmospheric Chemistry and Physics*, 16, 12875–
489 12896, <https://doi.org/10.5194/acp-16-12875-2016>, 2016.
- 490 Budisulistiorini, S. H., Canagaratna, M. R., Croteau, P. L., Marth, W. J., Baumann, K., Edgerton, E. S., Shaw, S. L.,
491 Knipping, E. M., Worsnop, D. R., Jayne, J. T., Gold, A., and Surratt, J. D.: Real-Time Continuous Characterization of
492 Secondary Organic Aerosol Derived from Isoprene Epoxydiols in Downtown Atlanta, Georgia, Using the Aerodyne Aerosol
493 Chemical Speciation Monitor, *Environ. Sci. Technol.*, 47, 5686–5694, <https://doi.org/10.1021/es400023n>, 2013.
- 494 Budisulistiorini, S. H., Canagaratna, M. R., Croteau, P. L., Baumann, K., Edgerton, E. S., Kollman, M. S., Ng, N. L., Verma,
495 V., Shaw, S. L., Knipping, E. M., Worsnop, D. R., Jayne, J. T., Weber, R. J., and Surratt, J. D.: Intercomparison of an
496 Aerosol Chemical Speciation Monitor (ACSM) with ambient fine aerosol measurements in downtown Atlanta, Georgia,
497 *Atmospheric Measurement Techniques*, 7, 1929–1941, <https://doi.org/10.5194/amt-7-1929-2014>, 2014.
- 498 Budisulistiorini, S. H., Li, X., Bairai, S. T., Renfro, J., Liu, Y., Liu, Y. J., McKinney, K. A., Martin, S. T., McNeill, V. F.,
499 Pye, H. O. T., Nenes, A., Neff, M. E., Stone, E. A., Mueller, S., Knote, C., Shaw, S. L., Zhang, Z., Gold, A., and Surratt, J.
500 D.: Examining the effects of anthropogenic emissions on isoprene-derived secondary organic aerosol formation during the
501 2013 Southern Oxidant and Aerosol Study (SOAS) at the Look Rock, Tennessee ground site, *Atmospheric Chemistry and
502 Physics*, 15, 8871–8888, <https://doi.org/10.5194/acp-15-8871-2015>, 2015.
- 503 Budisulistiorini, S. H., Baumann, K., Edgerton, E. S., Bairai, S. T., Mueller, S., Shaw, S. L., Knipping, E. M., Gold, A., and
504 Surratt, J. D.: Seasonal characterization of submicron aerosol chemical composition and organic aerosol sources in the
505 southeastern United States: Atlanta, Georgia, and Look Rock, Tennessee, *Atmospheric Chemistry and Physics*, 16, 5171–
506 5189, <https://doi.org/10.5194/acp-16-5171-2016>, 2016.
- 507 Canagaratna, M. R., Jayne, J. T., Ghertner, D. A., Herndon, S., Shi, Q., Jimenez, J. L., Silva, P. J., Williams, P., Lanni, T.,
508 Drewnick, F., Demerjian, K. L., Kolb, C. E., and Worsnop, D. R.: Chase Studies of Particulate Emissions from in-use New
509 York City Vehicles, *Aerosol Science and Technology*, 38, 555–573, <https://doi.org/10.1080/02786820490465504>, 2004.
- 510 Canagaratna, M. r., Jayne, J. t., Jimenez, J. l., Allan, J. d., Alfarra, M. r., Zhang, Q., Onasch, T. b., Drewnick, F., Coe, H.,
511 Middlebrook, A., Delia, A., Williams, L. r., Trimborn, A. m., Northway, M. j., DeCarlo, P. f., Kolb, C. e., Davidovits, P., and
512 Worsnop, D. r.: Chemical and microphysical characterization of ambient aerosols with the aerodyne aerosol mass
513 spectrometer, *Mass Spectrometry Reviews*, 26, 185–222, <https://doi.org/10.1002/mas.20115>, 2007.
- 514 Canonaco, F., Slowik, J. G., Baltensperger, U., and Prévôt, A. S. H.: Seasonal differences in oxygenated organic aerosol
515 composition: implications for emissions sources and factor analysis, *Atmospheric Chemistry and Physics*, 15, 6993–7002,
516 <https://doi.org/10.5194/acp-15-6993-2015>, 2015.
- 517 Carbone, S., Saarikoski, S., Frey, A., Reyes, F., Reyes, P., Castillo, M., Gramsch, E., Oyola, P., Jayne, J., Worsnop, D. R.,
518 and Hillamo, R.: Chemical Characterization of Submicron Aerosol Particles in Santiago de Chile, *Aerosol Air Qual. Res.*, 13,
519 462–473, <https://doi.org/10.4209/aaqr.2012.10.0261>, 2013.
- 520 Chhabra, P. S., Flagan, R. C., and Seinfeld, J. H.: Elemental analysis of chamber organic aerosol using an aerodyne high-
521 resolution aerosol mass spectrometer, *Atmospheric Chemistry and Physics*, 10, 4111–4131, <https://doi.org/10.5194/acp-10-4111-2010>, 2010.
- 523 Chirico, R., DeCarlo, P. F., Heringa, M. F., Tritscher, T., Richter, R., Prévôt, A. S. H., Dommen, J., Weingartner, E., Wehrle,
524 G., Gysel, M., Laborde, M., and Baltensperger, U.: Impact of aftertreatment devices on primary emissions and secondary
525 organic aerosol formation potential from in-use diesel vehicles: results from smog chamber experiments, *Atmospheric
526 Chemistry and Physics*, 10, 11545–11563, <https://doi.org/10.5194/acp-10-11545-2010>, 2010.



- 527 Claeys, M., Roberts, G., Mallet, M., Arndt, J., Sellegri, K., Sciare, J., Wenger, J., and Sauvage, B.: Optical, physical and
528 chemical properties of aerosols transported to a coastal site in the western Mediterranean: a focus on primary marine aerosols,
529 *Atmospheric Chemistry and Physics*, 17, 7891–7915, <https://doi.org/10.5194/acp-17-7891-2017>, 2017.
- 530 Cleveland, M. J., Ziemba, L. D., Griffin, R. J., Dibb, J. E., Anderson, C. H., Lefer, B., and Rappenglück, B.: Characterization
531 of urban aerosol using aerosol mass spectrometry and proton nuclear magnetic resonance spectroscopy, *Atmospheric
532 Environment*, 54, 511–518, <https://doi.org/10.1016/j.atmosenv.2012.02.074>, 2012.
- 533 Coggon, M. M., Sorooshian, A., Wang, Z., Metcalf, A. R., Frossard, A. A., Lin, J. J., Craven, J. S., Nenes, A., Jonsson, H. H.,
534 Russell, L. M., Flagan, R. C., and Seinfeld, J. H.: Ship impacts on the marine atmosphere: insights into the contribution of
535 shipping emissions to the properties of marine aerosol and clouds, *Atmospheric Chemistry and Physics*, 12, 8439–8458,
536 <https://doi.org/10.5194/acp-12-8439-2012>, 2012.
- 537 Collier, S., Zhou, S., Kuwayama, T., Forestieri, S., Brady, J., Zhang, M., Kleeman, M., Cappa, C., Bertram, T., and Zhang,
538 Q.: Organic PM Emissions from Vehicles: Composition, O/C Ratio, and Dependence on PM Concentration, *Aerosol Science
539 and Technology*, 49, 86–97, <https://doi.org/10.1080/02786826.2014.1003364>, 2015.
- 540 Crippa, M., El Haddad, I., Slowik, J. G., DeCarlo, P. F., Mohr, C., Heringa, M. F., Chirico, R., Marchand, N., Sciare, J.,
541 Baltensperger, U., and Prévôt, A. S. H.: Identification of marine and continental aerosol sources in Paris using high resolution
542 aerosol mass spectrometry, *Journal of Geophysical Research: Atmospheres*, 118, 1950–1963,
543 <https://doi.org/10.1002/jgrd.50151>, 2013.
- 544 Dall’Osto, M., Ovadnevaite, J., Ceburnis, D., Martin, D., Healy, R. M., O’Connor, I. P., Kourtchev, I., Sodeau, J. R.,
545 Wenger, J. C., and O’Dowd, C.: Characterization of urban aerosol in Cork city (Ireland) using aerosol mass spectrometry,
546 *Atmospheric Chemistry and Physics*, 13, 4997–5015, <https://doi.org/10.5194/acp-13-4997-2013>, 2013.
- 547 Day, D. A., Fry, J. L., Kang, H. G., Krechmer, J. E., Ayres, B. R., Keehan, N. I., Thompson, S. L., Hu, W., Campuzano-Jost,
548 P., Schroder, J. C., Stark, H., DeVault, M. P., Ziemann, P. J., Zarzana, K. J., Wild, R. J., Dubè, W. P., Brown, S. S., and
549 Jimenez, J. L.: Secondary Organic Aerosol Mass Yields from NO₃ Oxidation of α -Pinene and Δ -Carene: Effect of RO₂
550 Radical Fate, *J. Phys. Chem. A*, 126, 7309–7330, <https://doi.org/10.1021/acs.jpca.2c04419>, 2022.
- 551 De Gouw, J. and Jimenez, J. L.: Organic Aerosols in the Earth’s Atmosphere, *Environ. Sci. Technol.*, 43, 7614–7618,
552 <https://doi.org/10.1021/es9006004>, 2009.
- 553 DeCarlo, P. F., Kimmel, J. R., Trimborn, A., Northway, M. J., Jayne, J. T., Aiken, A. C., Gonin, M., Fuhrer, K., Horvath, T.,
554 Docherty, K. S., Worsnop, D. R., and Jimenez, J. L.: Field-Deployable, High-Resolution, Time-of-Flight Aerosol Mass
555 Spectrometer, *Anal. Chem.*, 78, 8281–8289, <https://doi.org/10.1021/ac061249n>, 2006.
- 556 Docherty, K. S., Aiken, A. C., Huffman, J. A., Ulbrich, I. M., DeCarlo, P. F., Sueper, D., Worsnop, D. R., Snyder, D. C.,
557 Peltier, R. E., Weber, R. J., Grover, B. D., Eatough, D. J., Williams, B. J., Goldstein, A. H., Ziemann, P. J., and Jimenez, J.
558 L.: The 2005 Study of Organic Aerosols at Riverside (SOAR-1): instrumental intercomparisons and fine particle
559 composition, *Atmospheric Chemistry and Physics*, 11, 12387–12420, <https://doi.org/10.5194/acp-11-12387-2011>, 2011.
- 560 Drewnick, F., Böttger, T., von der Weiden-Reinmüller, S.-L., Zorn, S. R., Klimach, T., Schneider, J., and Borrmann, S.:
561 Design of a mobile aerosol research laboratory and data processing tools for effective stationary and mobile field
562 measurements, *Atmospheric Measurement Techniques*, 5, 1443–1457, <https://doi.org/10.5194/amt-5-1443-2012>, 2012.
- 563 Elser, M., Huang, R.-J., Wolf, R., Slowik, J. G., Wang, Q., Canonaco, F., Li, G., Bozzetti, C., Daellenbach, K. R., Huang, Y.,
564 Zhang, R., Li, Z., Cao, J., Baltensperger, U., El-Haddad, I., and Prévôt, A. S. H.: New insights into PM_{2.5} chemical
565 composition and sources in two major cities in China during extreme haze events using aerosol mass spectrometry,
566 *Atmospheric Chemistry and Physics*, 16, 3207–3225, <https://doi.org/10.5194/acp-16-3207-2016>, 2016.
- 567 Fortenberry, C. F., Walker, M. J., Zhang, Y., Mitroo, D., Brune, W. H., and Williams, B. J.: Bulk and molecular-level
568 characterization of laboratory-aged biomass burning organic aerosol from oak leaf and heartwood fuels, *Atmospheric
569 Chemistry and Physics*, 18, 2199–2224, <https://doi.org/10.5194/acp-18-2199-2018>, 2018.
- 570 Fröhlich, R., Cubison, M. J., Slowik, J. G., Bukowiecki, N., Prévôt, A. S. H., Baltensperger, U., Schneider, J., Kimmel, J. R.,
571 Gonin, M., Rohner, U., Worsnop, D. R., and Jayne, J. T.: The ToF-ACSM: a portable aerosol chemical speciation monitor
572 with TOFMS detection, *Atmospheric Measurement Techniques*, 6, 3225–3241, <https://doi.org/10.5194/amt-6-3225-2013>,
573 2013.



- 574 Fröhlich, R., Crenn, V., Setyan, A., Belis, C. A., Canonaco, F., Favez, O., Riffault, V., Slowik, J. G., Aas, W., Aijälä, M.,
575 Alastuey, A., Artiñano, B., Bonnaire, N., Bozzetti, C., Bressi, M., Carbone, C., Coz, E., Croteau, P. L., Cubison, M. J., Esser-
576 Gietl, J. K., Green, D. C., Gros, V., Heikkinen, L., Herrmann, H., Jayne, J. T., Lunder, C. R., Minguillón, M. C., Močnik, G.,
577 O'Dowd, C. D., Ovadnevaite, J., Petralia, E., Poulain, L., Priestman, M., Ripoll, A., Sarda-Estève, R., Wiedensohler, A.,
578 Baltensperger, U., Sciare, J., and Prévôt, A. S. H.: ACTRIS ACSM intercomparison – Part 2: Intercomparison of ME-2
579 organic source apportionment results from 15 individual, co-located aerosol mass spectrometers, *Atmospheric Measurement*
580 *Techniques*, 8, 2555–2576, <https://doi.org/10.5194/amt-8-2555-2015>, 2015a.
- 581 Fröhlich, R., Cubison, M. J., Slowik, J. G., Bukowiecki, N., Canonaco, F., Croteau, P. L., Gysel, M., Henne, S., Herrmann,
582 E., Jayne, J. T., Steinbacher, M., Worsnop, D. R., Baltensperger, U., and Prévôt, A. S. H.: Fourteen months of on-line
583 measurements of the non-refractory submicron aerosol at the Jungfraujoch (3580 m a.s.l.) – chemical composition, origins
584 and organic aerosol sources, *Atmospheric Chemistry and Physics*, 15, 11373–11398, [https://doi.org/10.5194/acp-15-11373-](https://doi.org/10.5194/acp-15-11373-2015)
585 2015, 2015b.
- 586 Goldstein, A. H. and Galbally, I. E.: Known and unexplored organic constituents in the earth's atmosphere, *Environmental*
587 *science & technology*, 41, 1514–1521, 2007.
- 588 Hao, L. Q., Kortelainen, A., Romakkaniemi, S., Portin, H., Jaatinen, A., Leskinen, A., Komppula, M., Miettinen, P., Sueper,
589 D., Pajunoja, A., Smith, J. N., Lehtinen, K. E. J., Worsnop, D. R., Laaksonen, A., and Virtanen, A.: Atmospheric submicron
590 aerosol composition and particulate organic nitrate formation in a boreal forestland–urban mixed region, *Atmospheric*
591 *Chemistry and Physics*, 14, 13483–13495, <https://doi.org/10.5194/acp-14-13483-2014>, 2014.
- 592 Hayes, P. L., Ortega, A. M., Cubison, M. J., Froyd, K. D., Zhao, Y., Cliff, S. S., Hu, W. W., Toohey, D. W., Flynn, J. H.,
593 Lefer, B. L., Grossberg, N., Alvarez, S., Rappenglück, B., Taylor, J. W., Allan, J. D., Holloway, J. S., Gilman, J. B., Kuster,
594 W. C., de Gouw, J. A., Massoli, P., Zhang, X., Liu, J., Weber, R. J., Corrigan, A. L., Russell, L. M., Isaacman, G., Worton,
595 D. R., Kreisberg, N. M., Goldstein, A. H., Thalman, R., Waxman, E. M., Volkamer, R., Lin, Y. H., Surratt, J. D., Kleindienst,
596 T. E., Offenberg, J. H., Dusanter, S., Griffith, S., Stevens, P. S., Brioude, J., Angevine, W. M., and Jimenez, J. L.: Organic
597 aerosol composition and sources in Pasadena, California, during the 2010 CalNex campaign, *Journal of Geophysical*
598 *Research: Atmospheres*, 118, 9233–9257, <https://doi.org/10.1002/jgrd.50530>, 2013.
- 599 He, L.-Y., Lin, Y., Huang, X.-F., Guo, S., Xue, L., Su, Q., Hu, M., Luan, S.-J., and Zhang, Y.-H.: Characterization of high-
600 resolution aerosol mass spectra of primary organic aerosol emissions from Chinese cooking and biomass burning,
601 *Atmospheric Chemistry and Physics*, 10, 11535–11543, <https://doi.org/10.5194/acp-10-11535-2010>, 2010.
- 602 He, L.-Y., Huang, X.-F., Xue, L., Hu, M., Lin, Y., Zheng, J., Zhang, R., and Zhang, Y.-H.: Submicron aerosol analysis and
603 organic source apportionment in an urban atmosphere in Pearl River Delta of China using high-resolution aerosol mass
604 spectrometry, *Journal of Geophysical Research: Atmospheres*, 116, <https://doi.org/10.1029/2010JD014566>, 2011.
- 605 Heikkinen, L., Äijälä, M., Riva, M., Luoma, K., Dällenbach, K., Aalto, J., Aalto, P., Aliaga, D., Aurela, M., Keskinen, H.,
606 Makkonen, U., Rantala, P., Kulmala, M., Petäjä, T., Worsnop, D., and Ehn, M.: Long-term sub-micrometer aerosol chemical
607 composition in the boreal forest: inter- and intra-annual variability, *Atmospheric Chemistry and Physics*, 20, 3151–3180,
608 <https://doi.org/10.5194/acp-20-3151-2020>, 2020.
- 609 Heringa, M. F., DeCarlo, P. F., Chirico, R., Tritscher, T., Dommen, J., Weingartner, E., Richter, R., Wehrle, G., Prévôt, A. S.
610 H., and Baltensperger, U.: Investigations of primary and secondary particulate matter of different wood combustion
611 appliances with a high-resolution time-of-flight aerosol mass spectrometer, *Atmospheric Chemistry and Physics*, 11, 5945–
612 5957, <https://doi.org/10.5194/acp-11-5945-2011>, 2011.
- 613 Hu, W., Hu, M., Hu, W., Jimenez, J. L., Yuan, B., Chen, W., Wang, M., Wu, Y., Chen, C., Wang, Z., Peng, J., Zeng, L., and
614 Shao, M.: Chemical composition, sources, and aging process of submicron aerosols in Beijing: Contrast between summer and
615 winter, *Journal of Geophysical Research: Atmospheres*, 121, 1955–1977, <https://doi.org/10.1002/2015JD024020>, 2016.
- 616 Hu, W., Day, D. A., Campuzano-Jost, P., Nault, B. A., Park, T., Lee, T., Croteau, P., Canagaratna, M. R., Jayne, J. T.,
617 Worsnop, D. R., and Jimenez, J. L.: Evaluation of the New Capture Vaporizer for Aerosol Mass Spectrometers (AMS):
618 Elemental Composition and Source Apportionment of Organic Aerosols (OA), *ACS Earth Space Chem.*, 2, 410–421,
619 <https://doi.org/10.1021/acsearthspacechem.8b00002>, 2018a.
- 620 Hu, W., Day, D. A., Campuzano-Jost, P., Nault, B. A., Park, T., Lee, T., Croteau, P., Canagaratna, M. R., Jayne, J. T.,
621 Worsnop, D. R., and Jimenez, J. L.: Evaluation of the new capture vaporizer for aerosol mass spectrometers: Characterization
622 of organic aerosol mass spectra, *Aerosol Science and Technology*, 52, 725–739,



- 623 <https://doi.org/10.1080/02786826.2018.1454584>, 2018b.
- 624 Hu, W. W., Hu, M., Yuan, B., Jimenez, J. L., Tang, Q., Peng, J. F., Hu, W., Shao, M., Wang, M., Zeng, L. M., Wu, Y. S.,
625 Gong, Z. H., Huang, X. F., and He, L. Y.: Insights on organic aerosol aging and the influence of coal combustion at a
626 regional receptor site of central eastern China, *Atmospheric Chemistry and Physics*, 13, 10095–10112,
627 <https://doi.org/10.5194/acp-13-10095-2013>, 2013.
- 628 Hu, W. W., Campuzano-Jost, P., Palm, B. B., Day, D. A., Ortega, A. M., Hayes, P. L., Krechmer, J. E., Chen, Q., Kuwata,
629 M., Liu, Y. J., de Sá, S. S., McKinney, K., Martin, S. T., Hu, M., Budisulistiorini, S. H., Riva, M., Surratt, J. D., St. Clair, J.
630 M., Isaacman-Van Wertz, G., Yee, L. D., Goldstein, A. H., Carbone, S., Brito, J., Artaxo, P., de Gouw, J. A., Koss, A.,
631 Wisthaler, A., Mikoviny, T., Karl, T., Kaser, L., Jud, W., Hansel, A., Docherty, K. S., Alexander, M. L., Robinson, N. H.,
632 Coe, H., Allan, J. D., Canagaratna, M. R., Paulot, F., and Jimenez, J. L.: Characterization of a real-time tracer for isoprene
633 epoxydiols-derived secondary organic aerosol (IEPOX-SOA) from aerosol mass spectrometer measurements, *Atmospheric
634 Chemistry and Physics*, 15, 11807–11833, <https://doi.org/10.5194/acp-15-11807-2015>, 2015.
- 635 IPCC: Climate Change 2021: The Physical Science Basis. Contribution of Working Group I to the Sixth Assessment Report
636 of the Intergovernmental Panel on Climate Change, , In Press, <https://doi.org/10.1017/9781009157896>, 2021.
- 637 Jayne, J. T., Leard, D. C., Zhang, X., Davidovits, P., Smith, K. A., Kolb, C. E., and Worsnop, D. R.: Development of an
638 Aerosol Mass Spectrometer for Size and Composition Analysis of Submicron Particles, *Aerosol Science and Technology*, 33,
639 49–70, <https://doi.org/10.1080/027868200410840>, 2000.
- 640 Jimenez, J. L., Jayne, J. T., Shi, Q., Kolb, C. E., Worsnop, D. R., Yourshaw, I., Seinfeld, J. H., Flagan, R. C., Zhang, X.,
641 Smith, K. A., Morris, J. W., and Davidovits, P.: Ambient aerosol sampling using the Aerodyne Aerosol Mass Spectrometer,
642 *Journal of Geophysical Research: Atmospheres*, 108, <https://doi.org/10.1029/2001JD001213>, 2003.
- 643 Kampa, M. and Castanas, E.: Human health effects of air pollution, *Environmental Pollution*, 151, 362–367,
644 <https://doi.org/10.1016/j.envpol.2007.06.012>, 2008.
- 645 Katrib, Y., Martin, S. T., Hung, H.-M., Rudich, Y., Zhang, H., Slowik, J. G., Davidovits, P., Jayne, J. T., and Worsnop, D.
646 R.: Products and Mechanisms of Ozone Reactions with Oleic Acid for Aerosol Particles Having Core–Shell Morphologies, *J.
647 Phys. Chem. A*, 108, 6686–6695, <https://doi.org/10.1021/jp049759d>, 2004.
- 648 Kim, H., Zhang, Q., Bae, G.-N., Kim, J. Y., and Lee, S. B.: Sources and atmospheric processing of winter aerosols in Seoul,
649 Korea: insights from real-time measurements using a high-resolution aerosol mass spectrometer, *Atmospheric Chemistry and
650 Physics*, 17, 2009–2033, <https://doi.org/10.5194/acp-17-2009-2017>, 2017.
- 651 Kommula, S. M., Upasana, P., Sharma, A., Raj, S. S., Reyes-villegas, E., Liu, T., Allan, J. D., Jose, C., Pöhlker, M. L.,
652 Ravikrishna, R., Liu, P., Su, H., Martin, S. T., Pöschl, U., Mcfiggans, G., Coe, H., and Gunthe, S. S.: Chemical
653 Characterization and Source Apportionment of Organic Aerosols in the Coastal City of Chennai, India: Impact of Marine Air
654 Masses on Aerosol Chemical Composition and Potential for Secondary Organic Aerosol Formation, *ACS Earth Space
655 Chem.*, 5, 3197–3209, <https://doi.org/10.1021/acsearthspacechem.1c00276>, 2021.
- 656 Kroll, J. H., Ng, N. L., Murphy, S. M., Flagan, R. C., and Seinfeld, J. H.: Secondary organic aerosol formation from isoprene
657 photooxidation under high-NO_x conditions, *Geophysical Research Letters*, 32, <https://doi.org/10.1029/2005GL023637>, 2005.
- 658 Kroll, J. H., Ng, N. L., Murphy, S. M., Flagan, R. C., and Seinfeld, J. H.: Secondary Organic Aerosol Formation from
659 Isoprene Photooxidation, *Environ. Sci. Technol.*, 40, 1869–1877, <https://doi.org/10.1021/es0524301>, 2006.
- 660 Lambe, A. T., Onasch, T. B., Massoli, P., Croasdale, D. R., Wright, J. P., Ahern, A. T., Williams, L. R., Worsnop, D. R.,
661 Brune, W. H., and Davidovits, P.: Laboratory studies of the chemical composition and cloud condensation nuclei (CCN)
662 activity of secondary organic aerosol (SOA) and oxidized primary organic aerosol (OPOA), *Atmospheric Chemistry and
663 Physics*, 11, 8913–8928, <https://doi.org/10.5194/acp-11-8913-2011>, 2011.
- 664 Lambe, A. T., Onasch, T. B., Croasdale, D. R., Wright, J. P., Martin, A. T., Franklin, J. P., Massoli, P., Kroll, J. H.,
665 Canagaratna, M. R., Brune, W. H., Worsnop, D. R., and Davidovits, P.: Transitions from Functionalization to Fragmentation
666 Reactions of Laboratory Secondary Organic Aerosol (SOA) Generated from the OH Oxidation of Alkane Precursors,
667 *Environ. Sci. Technol.*, 46, 5430–5437, <https://doi.org/10.1021/es300274t>, 2012.
- 668 Lambe, A. T., Chhabra, P. S., Onasch, T. B., Brune, W. H., Hunter, J. F., Kroll, J. H., Cummings, M. J., Brogan, J. F.,
669 Parmar, Y., Worsnop, D. R., Kolb, C. E., and Davidovits, P.: Effect of oxidant concentration, exposure time, and seed



- 670 particles on secondary organic aerosol chemical composition and yield, *Atmos. Chem. Phys.*, 15, 3063–3075,
671 <https://doi.org/10.5194/acp-15-3063-2015>, 2015.
- 672 Lanz, V. A., Alfara, M. R., Baltensperger, U., Buchmann, B., Hueglin, C., and Prévôt, A. S. H.: Source apportionment of
673 submicron organic aerosols at an urban site by factor analytical modelling of aerosol mass spectra, *Atmospheric Chemistry
674 and Physics*, 7, 1503–1522, <https://doi.org/10.5194/acp-7-1503-2007>, 2007.
- 675 Lee, T., Choi, J., Lee, G., Ahn, J., Park, J. S., Atwood, S. A., Schurman, M., Choi, Y., Chung, Y., and Collett, J. L.:
676 Characterization of aerosol composition, concentrations, and sources at Baengnyeong Island, Korea using an aerosol mass
677 spectrometer, *Atmospheric Environment*, 120, 297–306, <https://doi.org/10.1016/j.atmosenv.2015.08.038>, 2015.
- 678 Li, Y. J., Yeung, J. W. T., Leung, T. P. I., Lau, A. P. S., and Chan, C. K.: Characterization of Organic Particles from Incense
679 Burning Using an Aerodyne High-Resolution Time-of-Flight Aerosol Mass Spectrometer, *Aerosol Science and Technology*,
680 46, 654–665, <https://doi.org/10.1080/02786826.2011.653017>, 2012.
- 681 Lim, C. Y., Hagan, D. H., Coggon, M. M., Koss, A. R., Sekimoto, K., de Gouw, J., Warneke, C., Cappa, C. D., and Kroll, J.
682 H.: Secondary organic aerosol formation from the laboratory oxidation of biomass burning emissions, *Atmospheric
683 Chemistry and Physics*, 19, 12797–12809, <https://doi.org/10.5194/acp-19-12797-2019>, 2019.
- 684 Loza, C. L., Chhabra, P. S., Yee, L. D., Craven, J. S., Flagan, R. C., and Seinfeld, J. H.: Chemical aging of *m*-xylene
685 secondary organic aerosol: laboratory chamber study, *Atmospheric Chemistry and Physics*, 12, 151–167,
686 <https://doi.org/10.5194/acp-12-151-2012>, 2012.
- 687 Loza, C. L., Craven, J. S., Yee, L. D., Coggon, M. M., Schwantes, R. H., Shiraiwa, M., Zhang, X., Schilling, K. A., Ng, N.
688 L., Canagaratna, M. R., Ziemann, P. J., Flagan, R. C., and Seinfeld, J. H.: Secondary organic aerosol yields of 12-carbon
689 alkanes, *Atmospheric Chemistry and Physics*, 14, 1423–1439, <https://doi.org/10.5194/acp-14-1423-2014>, 2014.
- 690 Marcolli, C., Canagaratna, M. R., Worsnop, D. R., Bahreini, R., de Gouw, J. A., Warneke, C., Goldan, P. D., Kuster, W. C.,
691 Williams, E. J., Lerner, B. M., Roberts, J. M., Meagher, J. F., Fehsenfeld, F. C., Marchewka, M., Bertman, S. B., and
692 Middlebrook, A. M.: Cluster Analysis of the Organic Peaks in Bulk Mass Spectra Obtained During the 2002 New England
693 Air Quality Study with an Aerodyne Aerosol Mass Spectrometer, *Atmospheric Chemistry and Physics*, 6, 5649–5666,
694 <https://doi.org/10.5194/acp-6-5649-2006>, 2006.
- 695 Michoud, V., Sciare, J., Sauvage, S., Dusanter, S., Léonardis, T., Gros, V., Kalogridis, C., Zannoni, N., Féron, A., Petit, J.-E.,
696 Crenn, V., Baisnée, D., Sarda-Estève, R., Bonnaire, N., Marchand, N., DeWitt, H. L., Pey, J., Colomb, A., Gheusi, F., Szidat,
697 S., Stavroulas, I., Borbon, A., and Locoge, N.: Organic carbon at a remote site of the western Mediterranean Basin: sources
698 and chemistry during the ChArMEx SOP2 field experiment, *Atmospheric Chemistry and Physics*, 17, 8837–8865,
699 <https://doi.org/10.5194/acp-17-8837-2017>, 2017.
- 700 Minguillón, M. C., Perron, N., Querol, X., Szidat, S., Fahrni, S. M., Alastuey, A., Jimenez, J. L., Mohr, C., Ortega, A. M.,
701 Day, D. A., Lanz, V. A., Wacker, L., Reche, C., Cusack, M., Amato, F., Kiss, G., Hoffer, A., Decesari, S., Moretti, F.,
702 Hillamo, R., Teinilä, K., Seco, R., Peñuelas, J., Metzger, A., Schallhart, S., Müller, M., Hansel, A., Burkhardt, J. F.,
703 Baltensperger, U., and Prévôt, A. S. H.: Fossil versus contemporary sources of fine elemental and organic carbonaceous
704 particulate matter during the DAURE campaign in Northeast Spain, *Atmospheric Chemistry and Physics*, 11, 12067–12084,
705 <https://doi.org/10.5194/acp-11-12067-2011>, 2011.
- 706 Minguillón, M. C., Ripoll, A., Pérez, N., Prévôt, A. S. H., Canonaco, F., Querol, X., and Alastuey, A.: Chemical
707 characterization of submicron regional background aerosols in the western Mediterranean using an Aerosol Chemical
708 Speciation Monitor, *Atmospheric Chemistry and Physics*, 15, 6379–6391, <https://doi.org/10.5194/acp-15-6379-2015>, 2015.
- 709 Modini, R. L., Frossard, A. A., Ahlm, L., Russell, L. M., Corrigan, C. E., Roberts, G. C., Hawkins, L. N., Schroder, J. C.,
710 Bertram, A. K., Zhao, R., Lee, A. K. Y., Abbatt, J. P. D., Lin, J., Nenes, A., Wang, Z., Wonaschütz, A., Sorooshian, A.,
711 Noone, K. J., Jonsson, H., Seinfeld, J. H., Toom-Sauntry, D., Macdonald, A. M., and Leaitch, W. R.: Primary marine aerosol-
712 cloud interactions off the coast of California, *Journal of Geophysical Research: Atmospheres*, 120, 4282–4303,
713 <https://doi.org/10.1002/2014JD022963>, 2015.
- 714 Mohr, C., Huffman, J. A., Cubison, M. J., Aiken, A. C., Docherty, K. S., Kimmel, J. R., Ulbrich, I. M., Hannigan, M., and
715 Jimenez, J. L.: Characterization of Primary Organic Aerosol Emissions from Meat Cooking, Trash Burning, and Motor
716 Vehicles with High-Resolution Aerosol Mass Spectrometry and Comparison with Ambient and Chamber Observations,
717 *Environ. Sci. Technol.*, 43, 2443–2449, <https://doi.org/10.1021/es8011518>, 2009.



- 718 Mohr, C., Richter, R., DeCarlo, P. F., Prévôt, A. S. H., and Baltensperger, U.: Spatial variation of chemical composition and
719 sources of submicron aerosol in Zurich during wintertime using mobile aerosol mass spectrometer data, *Atmospheric*
720 *Chemistry and Physics*, 11, 7465–7482, <https://doi.org/10.5194/acp-11-7465-2011>, 2011.
- 721 Mohr, C., DeCarlo, P. F., Heringa, M. F., Chirico, R., Slowik, J. G., Richter, R., Reche, C., Alastuey, A., Querol, X., Seco,
722 R., Peñuelas, J., Jiménez, J. L., Crippa, M., Zimmermann, R., Baltensperger, U., and Prévôt, A. S. H.: Identification and
723 quantification of organic aerosol from cooking and other sources in Barcelona using aerosol mass spectrometer data,
724 *Atmospheric Chemistry and Physics*, 12, 1649–1665, <https://doi.org/10.5194/acp-12-1649-2012>, 2012.
- 725 Murphy, S. M., Sorooshian, A., Kroll, J. H., Ng, N. L., Chhabra, P., Tong, C., Surratt, J. D., Knipping, E., Flagan, R. C., and
726 Seinfeld, J. H.: Secondary aerosol formation from atmospheric reactions of aliphatic amines, *Atmospheric Chemistry and*
727 *Physics*, 7, 2313–2337, <https://doi.org/10.5194/acp-7-2313-2007>, 2007.
- 728 Ng, N. L., Chhabra, P. S., Chan, A. W. H., Surratt, J. D., Kroll, J. H., Kwan, A. J., McCabe, D. C., Wennberg, P. O.,
729 Sorooshian, A., Murphy, S. M., Dalleska, N. F., Flagan, R. C., and Seinfeld, J. H.: Effect of NO_x level on secondary organic
730 aerosol (SOA) formation from the photooxidation of terpenes, *Atmospheric Chemistry and Physics*, 7, 5159–5174,
731 <https://doi.org/10.5194/acp-7-5159-2007>, 2007.
- 732 Ng, N. L., Kwan, A. J., Surratt, J. D., Chan, A. W. H., Chhabra, P. S., Sorooshian, A., Pye, H. O. T., Crounse, J. D.,
733 Wennberg, P. O., Flagan, R. C., and Seinfeld, J. H.: Secondary organic aerosol (SOA) formation from reaction of isoprene
734 with nitrate radicals (NO₃), *Atmospheric Chemistry and Physics*, 8, 4117–4140, <https://doi.org/10.5194/acp-8-4117-2008>,
735 2008.
- 736 Ng, N. L., Herndon, S. C., Trimborn, A., Canagaratna, M. R., Croteau, P. L., Onasch, T. B., Sueper, D., Worsnop, D. R.,
737 Zhang, Q., Sun, Y. L., and Jayne, J. T.: An Aerosol Chemical Speciation Monitor (ACSM) for Routine Monitoring of the
738 Composition and Mass Concentrations of Ambient Aerosol, *Aerosol Science and Technology*, 45, 780–794,
739 <https://doi.org/10.1080/02786826.2011.560211>, 2011.
- 740 Paatero, P. and Tapper, U.: Positive matrix factorization: A non-negative factor model with optimal utilization of error
741 estimates of data values, *Environmetrics*, 5, 111–126, <https://doi.org/10.1002/env.3170050203>, 1994.
- 742 Pandolfi, M., Querol, X., Alastuey, A., Jimenez, J. L., Jorba, O., Day, D., Ortega, A., Cubison, M. J., Comerón, A., Sicard,
743 M., Mohr, C., Prévôt, A. S. H., Minguillón, M. C., Pey, J., Baldasano, J. M., Burkhart, J. F., Seco, R., Peñuelas, J., van
744 Drooge, B. L., Artifano, B., Di Marco, C., Nemitz, E., Schallhart, S., Metzger, A., Hansel, A., Lorente, J., Ng, S., Jayne, J.,
745 and Szidat, S.: Effects of sources and meteorology on particulate matter in the Western Mediterranean Basin: An overview of
746 the DAURE campaign, *Journal of Geophysical Research: Atmospheres*, 119, 4978–5010,
747 <https://doi.org/10.1002/2013JD021079>, 2014.
- 748 Parworth, C., Fast, J., Mei, F., Shippert, T., Sivaraman, C., Tilp, A., Watson, T., and Zhang, Q.: Long-term measurements of
749 submicrometer aerosol chemistry at the Southern Great Plains (SGP) using an Aerosol Chemical Speciation Monitor
750 (ACSM), *Atmospheric Environment*, 106, 43–55, <https://doi.org/10.1016/j.atmosenv.2015.01.060>, 2015.
- 751 Petit, J.-E., Favez, O., Sciare, J., Crenn, V., Sarda-Estève, R., Bonnaire, N., Močnik, G., Dupont, J.-C., Haefelin, M., and
752 Leoz-Garziandia, E.: Two years of near real-time chemical composition of submicron aerosols in the region of Paris using an
753 Aerosol Chemical Speciation Monitor (ACSM) and a multi-wavelength Aethalometer, *Atmospheric Chemistry and Physics*,
754 15, 2985–3005, <https://doi.org/10.5194/acp-15-2985-2015>, 2015.
- 755 Phinney, L., Richard Leaitch, W., Lohmann, U., Boudries, H., Worsnop, D. R., Jayne, J. T., Toom-Sauntry, D., Wadleigh,
756 M., Sharma, S., and Shantz, N.: Characterization of the aerosol over the sub-arctic north east Pacific Ocean, *Deep Sea*
757 *Research Part II: Topical Studies in Oceanography*, 53, 2410–2433, <https://doi.org/10.1016/j.dsr2.2006.05.044>, 2006.
- 758 Pirjola, L., Niemi, J. V., Saarikoski, S., Aurela, M., Enroth, J., Carbone, S., Saarnio, K., Kuuluvainen, H., Kousa, A.,
759 Rönkkö, T., and Hillamo, R.: Physical and chemical characterization of urban winter-time aerosols by mobile measurements
760 in Helsinki, Finland, *Atmospheric Environment*, 158, 60–75, <https://doi.org/10.1016/j.atmosenv.2017.03.028>, 2017.
- 761 Ramanathan, V., Crutzen, P. J., Kiehl, J. T., and Rosenfeld, D.: Aerosols, Climate, and the Hydrological Cycle, *Science*, 294,
762 2119–2124, <https://doi.org/10.1126/science.1064034>, 2001.
- 763 Rattanavaraha, W., Canagaratna, M. R., Budisulistiorini, S. H., Croteau, P. L., Baumann, K., Canonaco, F., Prevot, A. S. H.,
764 Edgerton, E. S., Zhang, Z., Jayne, J. T., Worsnop, D. R., Gold, A., Shaw, S. L., and Surratt, J. D.: Source apportionment of
765 submicron organic aerosol collected from Atlanta, Georgia, during 2014–2015 using the aerosol chemical speciation monitor



- 766 (ACSM), *Atmospheric Environment*, 167, 389–402, <https://doi.org/10.1016/j.atmosenv.2017.07.055>, 2017.
- 767 Reyes-Villegas, E., Green, D. C., Priestman, M., Canonaco, F., Coe, H., Prévôt, A. S. H., and Allan, J. D.: Organic aerosol
768 source apportionment in London 2013 with ME-2: exploring the solution space with annual and seasonal analysis,
769 *Atmospheric Chemistry and Physics*, 16, 15545–15559, <https://doi.org/10.5194/acp-16-15545-2016>, 2016.
- 770 Ripoll, A., Minguillón, M. C., Pey, J., Jimenez, J. L., Day, D. A., Sosedova, Y., Canonaco, F., Prévôt, A. S. H., Querol, X.,
771 and Alastuey, A.: Long-term real-time chemical characterization of submicron aerosols at Montsec (southern Pyrenees, 1570
772 m a.s.l.), *Atmospheric Chemistry and Physics*, 15, 2935–2951, <https://doi.org/10.5194/acp-15-2935-2015>, 2015.
- 773 Riva, M., Budisulistiorini, S. H., Chen, Y., Zhang, Z., D’Ambro, E. L., Zhang, X., Gold, A., Turpin, B. J., Thornton, J. A.,
774 Canagaratna, M. R., and Surratt, J. D.: Chemical Characterization of Secondary Organic Aerosol from Oxidation of Isoprene
775 Hydroxyhydroperoxides, *Environ. Sci. Technol.*, 50, 9889–9899, <https://doi.org/10.1021/acs.est.6b02511>, 2016.
- 776 Robinson, E. S., Gu, P., Ye, Q., Li, H. Z., Shah, R. U., Apte, J. S., Robinson, A. L., and Presto, A. A.: Restaurant Impacts on
777 Outdoor Air Quality: Elevated Organic Aerosol Mass from Restaurant Cooking with Neighborhood-Scale Plume Extents,
778 *Environ. Sci. Technol.*, 52, 9285–9294, <https://doi.org/10.1021/acs.est.8b02654>, 2018.
- 779 Saarikoski, S., Carbone, S., Decesari, S., Giulianelli, L., Angelini, F., Canagaratna, M., Ng, N. L., Trimborn, A., Facchini, M.
780 C., Fuzzi, S., Hillamo, R., and Worsnop, D.: Chemical characterization of springtime submicrometer aerosol in Po Valley,
781 Italy, *Atmospheric Chemistry and Physics*, 12, 8401–8421, <https://doi.org/10.5194/acp-12-8401-2012>, 2012.
- 782 Sage, A. M., Weitkamp, E. A., Robinson, A. L., and Donahue, N. M.: Evolving mass spectra of the oxidized component of
783 organic aerosol: results from aerosol mass spectrometer analyses of aged diesel emissions, *Atmospheric Chemistry and
784 Physics*, 8, 1139–1152, <https://doi.org/10.5194/acp-8-1139-2008>, 2008.
- 785 Schlag, P., Kiendler-Scharr, A., Blom, M. J., Canonaco, F., Henzing, J. S., Moerman, M., Prévôt, A. S. H., and Holzinger, R.:
786 Aerosol source apportionment from 1-year measurements at the CESAR tower in Cabauw, the Netherlands, *Atmospheric
787 Chemistry and Physics*, 16, 8831–8847, <https://doi.org/10.5194/acp-16-8831-2016>, 2016.
- 788 Schneider, J., Weimer, S., Drewnick, F., Borrmann, S., Helas, G., Gwaze, P., Schmid, O., Andreae, M. O., and Kirchner, U.:
789 Mass spectrometric analysis and aerodynamic properties of various types of combustion-related aerosol particles,
790 *International Journal of Mass Spectrometry*, 258, 37–49, <https://doi.org/10.1016/j.ijms.2006.07.008>, 2006.
- 791 Setyan, A., Zhang, Q., Merkel, M., Knighton, W. B., Sun, Y., Song, C., Shilling, J. E., Onasch, T. B., Herndon, S. C.,
792 Worsnop, D. R., Fast, J. D., Zaveri, R. A., Berg, L. K., Wiedensohler, A., Flowers, B. A., Dubey, M. K., and Subramanian,
793 R.: Characterization of submicron particles influenced by mixed biogenic and anthropogenic emissions using high-resolution
794 aerosol mass spectrometry: results from CARES, *Atmospheric Chemistry and Physics*, 12, 8131–8156,
795 <https://doi.org/10.5194/acp-12-8131-2012>, 2012.
- 796 Shilling, J. E., Pekour, M. S., Fortner, E. C., Artaxo, P., de Sá, S., Hubbe, J. M., Longo, K. M., Machado, L. A. T., Martin, S.
797 T., Springston, S. R., Tomlinson, J., and Wang, J.: Aircraft observations of the chemical composition and aging of aerosol in
798 the Manaus urban plume during GoAmazon 2014/5, *Atmospheric Chemistry and Physics*, 18, 10773–10797,
799 <https://doi.org/10.5194/acp-18-10773-2018>, 2018.
- 800 Stein, S. E. and Scott, D. R.: Optimization and testing of mass spectral library search algorithms for compound identification,
801 *J. Am. Soc. Spectrom.*, 5, 859–866, [https://doi.org/10.1016/1044-0305\(94\)87009-8](https://doi.org/10.1016/1044-0305(94)87009-8), 1994.
- 802 Struckmeier, C., Drewnick, F., Fachinger, F., Gobbi, G. P., and Borrmann, S.: Atmospheric aerosols in Rome, Italy: sources,
803 dynamics and spatial variations during two seasons, *Atmospheric Chemistry and Physics*, 16, 15277–15299,
804 <https://doi.org/10.5194/acp-16-15277-2016>, 2016.
- 805 Sueper: <https://cires1.colorado.edu/jimenez-group/ToFAMSResources/ToFSoftware/>, last access: 17 January 2021.
- 806 Sun, Y., Xu, W., Zhang, Q., Jiang, Q., Canonaco, F., Prévôt, A. S. H., Fu, P., Li, J., Jayne, J., Worsnop, D. R., and Wang, Z.:
807 Source apportionment of organic aerosol from 2-year highly time-resolved measurements by an aerosol chemical speciation
808 monitor in Beijing, China, *Atmospheric Chemistry and Physics*, 18, 8469–8489, <https://doi.org/10.5194/acp-18-8469-2018>,
809 2018.
- 810 Sun, Y.-L., Zhang, Q., Schwab, J. J., Demerjian, K. L., Chen, W.-N., Bae, M.-S., Hung, H.-M., Hogrefe, O., Frank, B.,
811 Rattigan, O. V., and Lin, Y.-C.: Characterization of the sources and processes of organic and inorganic aerosols in New York



- 812 city with a high-resolution time-of-flight aerosol mass spectrometer, *Atmospheric Chemistry and Physics*, 11, 1581–1602,
813 <https://doi.org/10.5194/acp-11-1581-2011>, 2011.
- 814 Takegawa, N., Miyakawa, T., Kawamura, K., and Kondo, Y.: Contribution of Selected Dicarboxylic and ω -Oxocarboxylic
815 Acids in Ambient Aerosol to the m/z 44 Signal of an Aerodyne Aerosol Mass Spectrometer, *Aerosol Science and*
816 *Technology*, 41, 418–437, <https://doi.org/10.1080/02786820701203215>, 2007.
- 817 Tiitta, P., Vakkari, V., Croteau, P., Beukes, J. P., van Zyl, P. G., Josipovic, M., Venter, A. D., Jaars, K., Pienaar, J. J., Ng, N.
818 L., Canagaratna, M. R., Jayne, J. T., Kerminen, V.-M., Kokkola, H., Kulmala, M., Laaksonen, A., Worsnop, D. R., and
819 Laakso, L.: Chemical composition, main sources and temporal variability of PM₁ aerosols in southern African grassland,
820 *Atmospheric Chemistry and Physics*, 14, 1909–1927, <https://doi.org/10.5194/acp-14-1909-2014>, 2014.
- 821 Ulbrich, I. M., Canagaratna, M. R., Zhang, Q., Worsnop, D. R., and Jimenez, J. L.: Interpretation of organic components
822 from Positive Matrix Factorization of aerosol mass spectrometric data, *Atmospheric Chemistry and Physics*, 9, 2891–2918,
823 <https://doi.org/10.5194/acp-9-2891-2009>, 2009.
- 824 Wang, X., Williams, B. J., Wang, X., Tang, Y., Huang, Y., Kong, L., Yang, X., and Biswas, P.: Characterization of organic
825 aerosol produced during pulverized coal combustion in a drop tube furnace, *Atmospheric Chemistry and Physics*, 13, 10919–
826 10932, <https://doi.org/10.5194/acp-13-10919-2013>, 2013.
- 827 Weimer, S., Alfarra, M. R., Schreiber, D., Mohr, M., Prévôt, A. S. H., and Baltensperger, U.: Organic aerosol mass spectral
828 signatures from wood-burning emissions: Influence of burning conditions and wood type, *Journal of Geophysical Research:*
829 *Atmospheres*, 113, <https://doi.org/10.1029/2007JD009309>, 2008.
- 830 Xu, J., Zhang, Q., Chen, M., Ge, X., Ren, J., and Qin, D.: Chemical composition, sources, and processes of urban aerosols
831 during summertime in northwest China: insights from high-resolution aerosol mass spectrometry, *Atmospheric Chemistry*
832 *and Physics*, 14, 12593–12611, <https://doi.org/10.5194/acp-14-12593-2014>, 2014.
- 833 Xu, L., Suresh, S., Guo, H., Weber, R. J., and Ng, N. L.: Aerosol characterization over the southeastern United States using
834 high-resolution aerosol mass spectrometry: spatial and seasonal variation of aerosol composition and sources with a focus on
835 organic nitrates, *Atmospheric Chemistry and Physics*, 15, 7307–7336, <https://doi.org/10.5194/acp-15-7307-2015>, 2015.
- 836 Young, D. E., Kim, H., Parworth, C., Zhou, S., Zhang, X., Cappa, C. D., Seco, R., Kim, S., and Zhang, Q.: Influences of
837 emission sources and meteorology on aerosol chemistry in a polluted urban environment: results from DISCOVER-AQ
838 California, *Atmospheric Chemistry and Physics*, 16, 5427–5451, <https://doi.org/10.5194/acp-16-5427-2016>, 2016.
- 839 Zhang, Q., Alfarra, M. R., Worsnop, D. R., Allan, J. D., Coe, H., Canagaratna, M. R., and Jimenez, J. L.: Deconvolution and
840 Quantification of Hydrocarbon-like and Oxygenated Organic Aerosols Based on Aerosol Mass Spectrometry, *Environ. Sci.*
841 *Technol.*, 39, 4938–4952, <https://doi.org/10.1021/es0485681>, 2005.
- 842 Zhang, Q., Jimenez, J. L., Canagaratna, M. R., Ulbrich, I. M., Ng, N. L., Worsnop, D. R., and Sun, Y.: Understanding
843 atmospheric organic aerosols via factor analysis of aerosol mass spectrometry: a review, *Anal Bioanal Chem*, 401, 3045–
844 3067, <https://doi.org/10.1007/s00216-011-5355-y>, 2011.
- 845 Aerosol Mass Spectrometry (AMS) Global Database: [https://sites.google.com/site/amsglobaldatabase/urban-down-](https://sites.google.com/site/amsglobaldatabase/urban-downwind/montseny-spain)
846 [wind/montseny-spain](https://sites.google.com/site/amsglobaldatabase/urban-downwind/montseny-spain), last access: 23 December 2022.
- 847 Zhang, Y., Du, W., Wang, Y., Wang, Q., Wang, H., Zheng, H., Zhang, F., Shi, H., Bian, Y., Han, Y., Fu, P., Canonaco, F.,
848 Prévôt, A. S. H., Zhu, T., Wang, P., Li, Z., and Sun, Y.: Aerosol chemistry and particle growth events at an urban downwind
849 site in North China Plain, *Atmospheric Chemistry and Physics*, 18, 14637–14651, [https://doi.org/10.5194/acp-18-14637-](https://doi.org/10.5194/acp-18-14637-2018)
850 2018, 2018.
- 851 Zhao, Q., Huo, J., Yang, X., Fu, Q., Duan, Y., Liu, Y., Lin, Y., and Zhang, Q.: Chemical characterization and source
852 identification of submicron aerosols from a year-long real-time observation at a rural site of Shanghai using an Aerosol
853 Chemical Speciation Monitor, *Atmospheric Research*, 246, 105154, <https://doi.org/10.1016/j.atmosres.2020.105154>, 2020.
- 854 Zorn, S. R., Drewnick, F., Schott, M., Hoffmann, T., and Borrmann, S.: Characterization of the South Atlantic marine
855 boundary layer aerosol using an aerodyne aerosol mass spectrometer, *Atmospheric Chemistry and Physics*, 8, 4711–4728,
856 <https://doi.org/10.5194/acp-8-4711-2008>, 2008.